بسم الله الرحمن الرحيم

Car Accident Reconstruction

By

Fadi Younis Alama

Supervisor: Dr. Diya Arafah

Submitted to the College of Engineering

in partial fulfillment of the requirements for the degree of

Bachelor degree in Automotive Engineering

Palestine Polytechnic University

Dec 2015

Palestine Polytechnic University

Collage of Engineering and Technology

Mechanical Engineering Department

Hebron - Palestine

Project name

Car Accident Reconstruction

Project team

Fadi Younis Alama

According to the project supervisor and the examiner committee members, this project is submitted to the Department of Mechanical Engineering at the College of Engineering and Technology in partial fulfillment of the requirements for the Bachelor degree in Automotive Engineering

Supervisor signature

....

Committee members signature

....

Department Head signature

....

Dedication

To our Families ⋯ For their support

To our Teachers ⋯ For help us until the end

To our friends ⋯ Who give us positive sentiment

To oppressed people throughout the world and their struggle for social justice and egalitarianism

To our great Palestine

To my supervisor Dr. Diya Arafah

To all who made this work is possible

Fadi Younis Alama

Acknowledgment

I would like to express my gratitude for everyone who helps me during the graduation project, starting with endless thanks for my supervisor Dr. Diya Arafah who didn't keep any effort in encouraging me to do a great job, providing me with valuable information and advices to be better each time. Thanks for the continuous support and kind communication which great effect regarding to feel interesting about what I am working on.

Finally thanks are extended to the "Automotive and Mechanical society" for the beneficial lectures provided.

Abstract

Car accident is one of the most important problems, because sometimes the stories we took from the drivers couldn't determine the real cause of the accident, sometimes it is because one of the drivers, and in other times it is because of the environment (like weather, invisibility ,etc) or because of car systems malfunctions. A reliable method is needed to calculate and simulate the accident based on the data collected from the accident site, in order to predict the real cause of the accident. Several methods are used in car accident reconstruction (such as energy method, linear momentum), in the present study both the conservation of linear momentum and the conservation of energy used to reconstruct car to car accident. The principle will be applied on a case study as well.

حوادث السيارات من أكثر المشاكل أهمية، وذلك لعدم مقدرة المحققين من التوصل لإجابات صحيحة من طرفي الحادث، سواء كانوا سائقين أو شركات التأمين الخاصة بأصحاب المركبات. أحيانا يكون السبب الرئيسي لوقوع الحادث هو السائق، وفي أحيان أخرى تكون الظروف المحيطة هي السبب مثل الطقس وحالة الطريق ، أو قد تكون مشاكل فنية في احدى انظمة المركبة. لذلك نحن بحاجة لطريقة فعالة لحساب واعادة بناء مجريات الحادث بناءً على المعلومات التي يتم جمعها من موقع الحادث، وذلك لتوقع السبب الرئيسي لوقوع الحادث. عدة طرق يتم استعمالها في هذا المجال ومن اهمها نظرية حفظ الطاقة ونظرية حفظ الزخم الخطي . في هذا المشروع سيتم دراسة كلاً من نظرية حفظ الزخم الخطي و نظرية حفظ الطاقة لاعادة بناء مجريات الحادث، كما سيتم تطبيقها على نموذج من حوادث السيارات.

CONTENTS

LIST OF TABLES

LIST OF FIGURES

CHAPTER 1

INTRODUCTION

Chapter 1

Introduction

1.1 Overview

In the early decades of the 1900s, automotive engineering went into invention and design that would yield faster, comfortable and more reliable vehicles. These fast vehicles increased the risk of dangerous accidents (fatal).

In October 1904; the first automobile accident (non-fatal) was in New Zealand, Captain Subritzky's car collides with a tramcar in Hobson Street.
Then in September 1906; the first automobile fatality in New Zealand, Janet Meikle (Mrs John Meikle) aged 36, died after an accident in a car she was driving[1].

According to the association for safety international road travel nearly 1.3 million people die in road crashes each year, on average 3287 deaths a day[2]. Figure 1.1 shows the statistics of the fatality due to car accident world wide in each yaer. This huge number of accidents needs investigation in order to determine the real cause of accident. This project has been chosen to support car accident reconstruction in Palestine and will serve as the nucleus of car accident research in Palestine.

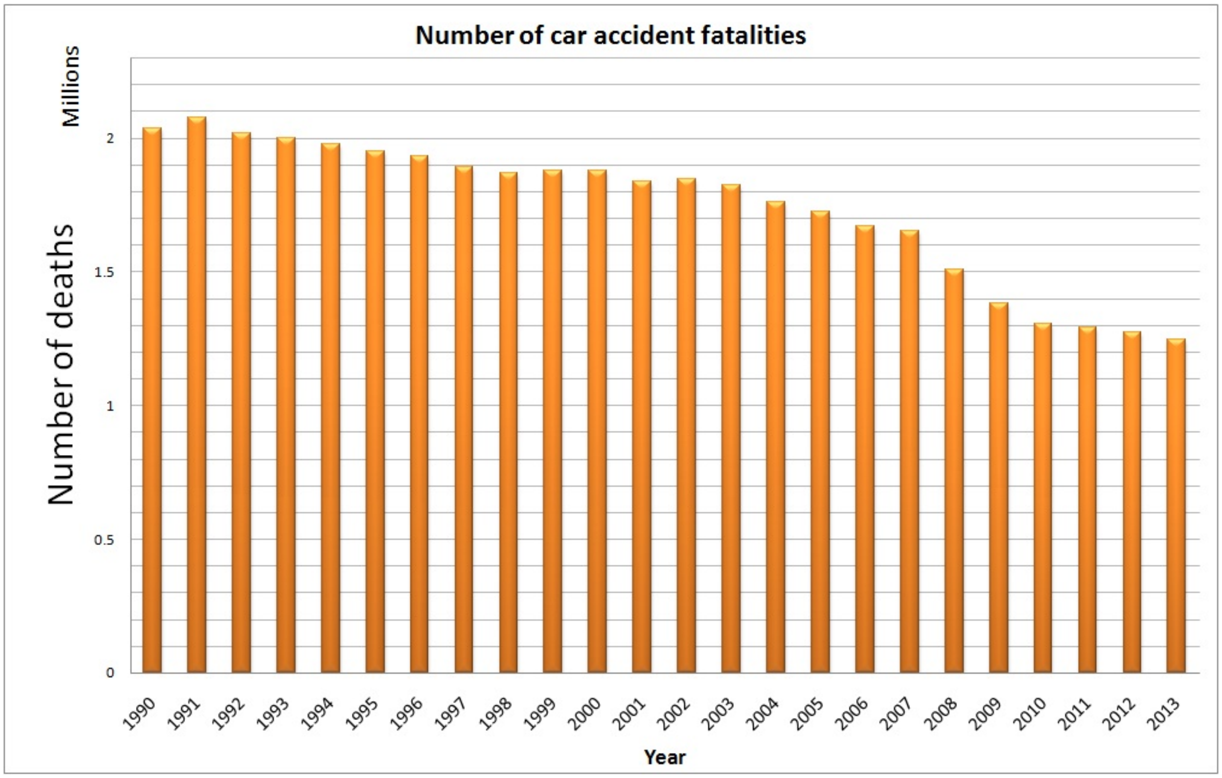

Figure 1.1: Number of car accident fatalities world wide[3]

1.2 Importance of the project

When an accident happens investigators of the police and the insurance companies come to the site and collect all the evidences they could find, then they try to reconstruct the accident using the evidences and the knowledge of physics and mechanical engineering science, to predict on who the blame is. And because of the uncertainty of the stories we could take from the drivers, we need these knowledge of engineering and physics, to have a closer prediction to real situation.

Car accident investigation will give a good feedback, that will help the insurance companies and the police; as well as engineers to make some modifications on the vehicles or on the roads to prevent future accidents.

1.3 Motivation

It is very important to know on who the blame is, because the judge needs to make his judgment. Therefore, as automotive engineers, it's our mission to calculate and predict how the accident happened. Moreover, there are some companies around the world that make these calculations by their own software, they sell these programs to the insurance companies and the police in a very large price. So why do not we make these programs?

1.4 Project Objectives

The main objective of this project is to implement the physical equations, tools and factors that needed to reconstruct car accident. A case study of real car accident will be used as verification example of the proposed method.

1.5 Methodology

In this project analytical methodology will be used. At the first we will study and implement the equations to reach the final equations that could be needed for a simple car accident reconstruction. Then the proposed method will be applied on case study as verification example.

1.6 Time plan

In this section the tasks and time tables will be determined as shown below:

Table 1.1: Tasks description

Task ID	**Task Description**
T1	Literature review
T2	Learning on Latex program
T3	Conservation of linear momentum and Energy methods
T4	Writing the book
T5	Preparing the 1^{st} semester presentation
T6	Building the program code
T7	Collecting data of case study
T8	Application of the proposed method on case study
T9	Writing the final book
T10	Preparing the final presentation

Table 1.2: Time table

1^{st} semester															
Task/Week	**1**	**2**	**3**	**4**	**5**	**6**	**7**	**8**	**9**	**10**	**11**	**12**	**13**	**14**	**15**
T1															
T2															
T3															
T4															
T5															
2^{nd} semester															
Task/Week	**16**	**17**	**18**	**19**	**20**	**21**	**22**	**23**	**24**	**25**	**26**	**27**	**28**	**29**	**30**
T6															
T7															
T8															
T9															
T10															

CHAPTER 2

CAR ACCIDENT COLLISION ANALYSIS

Chapter 2

Car accident collision analysis

2.1 Introduction

There are many methods used in car accident reconstruction such as the energy method and the linear momentum. The Conservation of Energy predicts car speed based on the deformation level happened due to the collision and it could be combined with conservation of linear momentum in particular cases where the available information from the accident site is not enough (such as there is no skid marks). In the present chapter the concept of collision and linear momentum and conservation of energy will be reviewed. And the application of conservation of linear momentum and conservation of energy to car accident will be discussed.

The basic classification of collisions are co-linear and non-co-linear based on physics classification. The co-linear collision means that it happens in one dimension. On the other hand, non-co-linear collision means that it happens in two dimensions or more.

Furthermore, there are another classifications, like the number of cars that enters the accident, and the direction of the accident, etc. Each kind of these has it's own factors that affect the result of the collision.

Car accident can happen in many situations, and if these classification factors combined together, between physics and mechanical engineering, car accident could be classified as shown below:

1) **Rear-end collision:** this type of collision happens when one car crashes into a car in front of it. Rear-endings can be caused by sudden deceleration (slowing down or braking) by the first car, or when the following car accelerates more rapidly than the car in front of it, as shown in figure 2.1.

Figure 2.1: Rear-end collision

2) **Side-impact collision:** also called a "T-bone" collision, or "broadsided," this occurs when the side of a car is impacted by the front or rear of another car or a fixed object, as shown in figure 2.2.

Figure 2.2: Side-impact collision

3) **Side-swipe collision:** this type occurs when the sides of two parallel cars touch and "swipe" each other, as shown in figure 2.3.

Figure 2.3: Side-swipe collision

4) **Rollover collision:** this occurs when a car flips over onto its side or roof. Rollovers are often caused by a sharp turn at high speed, as shown in figure 2.4. And this is a very dangerous collision.

Figure 2.4: Rollover collision

5) **Head-on collision:** this occurs when the front ends of two cars hit each other. Head-on collisions are often fatal, as shown in figure 2.5.

Figure 2.5: Head-on collision

6) **Single car collision:** this occurs when only one car is involved. In some cases a car strikes other objects such as poles, trees, fire hydrants, walls and may involve innocent pedestrian. Those accidents often result in property damage and personal injury, as shown in figure 2.6.

Figure 2.6: Single car collision

7) **Multi-car collision:** these accidents involving many cars. Usually they occur on highways or freeways. They are one of the deadliest kinds of traffic accidents, as shown in figure 2.7.

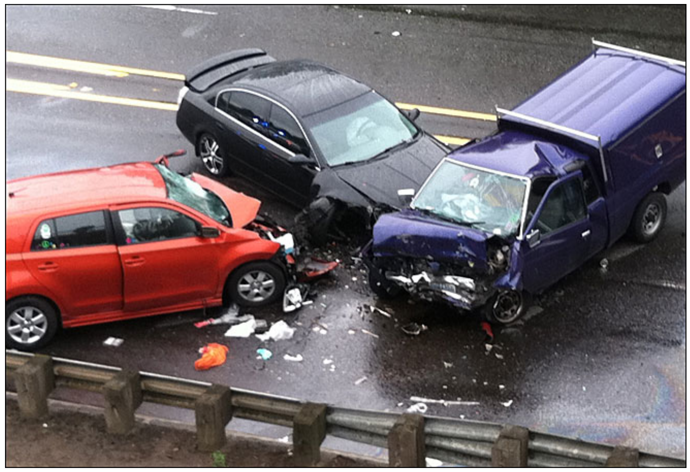

Figure 2.7: Multi-car collision

2.2 Linear Momentum and laws of motion

The Conservation of Linear Momentum (COLM) is one of the most used methods in car accident reconstruction[4]. Linear momentum was described 300 years ago by Sir Isaac; it is the product of the mass and velocity of an object. For example if there is a heavy mass moving rapidly, that means that it have a big momentum, this needs big force to make this mass go up to that speed. Like velocity, linear momentum is a vector quantity. So for accident reconstruction, we have two cars each one have its own mass and velocity. And any change in the mass or the velocity will change the path and trend of the accident, so linear momentum is a powerful tool in car accident reconstruction. As we know, linear momentum defined as:

$$M = m \cdot v \tag{2.1}$$

Where M is the momentum and m is the mass and v is the velocity. So momentum's direction is along to the velocity. And its SI unit is $Kg.m/sec$.

Newton's second law defined as when viewed from an inertial reference frame, the acceleration of an object is directly proportional to the net force acting on it and inversely proportional to its mass[5]. Which can be stated as:

$$F = m \cdot a \tag{2.2}$$

Where
F is the force acting on a body in N
m is the mass of the body in kg
a is the acceleration of the body in m/s^2

We know that acceleration defined as the change of velocity over the change in time so we can rewrite Newton's second law as:

$$F = m \cdot \left(\frac{\Delta V}{\Delta t} \right) \tag{2.3}$$

And if we rearrange terms, we find that:

$$F \cdot \Delta t = m \cdot \Delta V \tag{2.4}$$

So the force multiplied by the time equals the product of the mass and its change in velocity. The left hand of equation 2.4 known as the impulse and the right hand term is the change in momentum.

The Conservation of Linear Momentum (COLM) defined as whenever two or more particles in an isolated system interact, the total momentum of the system remains constant[5]. So if we assume two particles moving with velocities V_1 and V_2 and having masses of m_1 and m_2 respectively, and these particles are in a linear collision, then after collision they will have velocities as V_3 and V_4 , as shown in figure 2.8

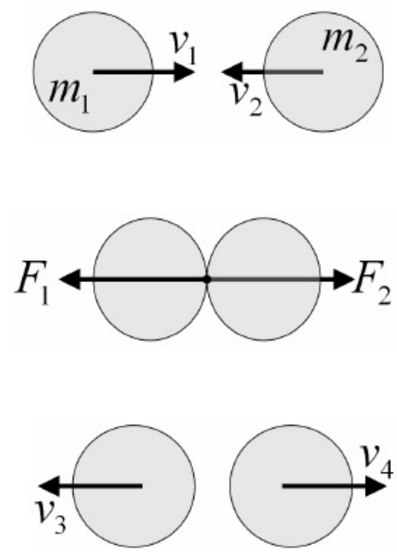

Figure 2.8: Two particles collide

Newton's third law says when one body exerts a force on a second body; the second body simultaneously exerts a force equal in magnitude and opposite in direction on the first body[5]. If we rearrange Newton's laws and substitute the second law in the third law we will get that:

$$m_1 \cdot a_1 = -m_2 \cdot a_2 \tag{2.5}$$

And by using the definition of the acceleration that we discussed we get:

$$m_1 \cdot \left(\frac{\Delta V_1}{\Delta t}\right) = m_2 \cdot \left(\frac{\Delta V_2}{\Delta t}\right) \tag{2.6}$$

By canceling the change of time from equation 2.6 and substitute the change in velocity as

$$\Delta V_1 = V_3 - V_1 \tag{2.7a}$$

$$\Delta V_2 = V_4 - V_2 \tag{2.7b}$$

and rearrange it to get equation 2.8 as shown below:

$$m_1 V_1 + m_2 V_2 = m_1 V_3 + m_2 V_4 \tag{2.8}$$

In equation 2.8 the left side represents the total momentum that carried in the system of the two particles or cars in our study just before the collision, and the right side represents the total momentum that carried out the system just after the collision.

2.3 Applying COLM to car accident collision

The system in this case is the accident of two cars, so there are two kinds of forces in this system. The first one is the force that each car apply on the other and this called the internal forces. For a typical accident, the internal forces are in the 200 kN range. The second one is the force that the tire and aerodynamics apply on the car, this called the external forces. The tire forces are in the 10 kN range, and the aerodynamics is much smaller than this, so the external forces (tires and aerodynamics forces), used to be neglect in conservation of linear momentum[4].

So by using conservation of linear momentum on a typical car accident, which means on the internal forces only, the total momentum going into the impact will equal the total momentum leaving the impact, as shown in equation 2.9.

$$\sum M_{in} = \sum M_{out} \tag{2.9}$$

Also the change of momentum of the first car equals the change of momentum of the second car, but in the opposite direction. This can be written as shown in equation 2.10.

$$\Delta M_1 = -\Delta M_2 \tag{2.10}$$

So the change of momentum for each car can be written as shown in equation 2.11.

$$\Delta M_1 = M_3 - M_1 \tag{2.11a}$$

$$\Delta M_2 = M_4 - M_2 \tag{2.11b}$$

Where

M_1 is the pre-impact momentum of car 1

M_2 is the pre-impact momentum of car 2

M_3 is the post-impact momentum of car 1

M_4 is the post-impact momentum of car 2

Now by substitute equation 2.11 in equation 2.10, and rearrange it to reach equation 2.12 as shown below.

$$M_1 + M_2 = M_3 + M_4 \tag{2.12}$$

Now by substitute equation 2.1 in equation 2.12, we will get equation 2.13 as shown below.

$$m_1V_1 + m_2V_2 = m_1V_3 + m_2V_4 \tag{2.13}$$

Where

m_1 is the mass of car 1 in Kg

m_2 is the mass of car 2 in Kg

V_1 is the pre-impact velocity of car 1 in m/s

V_2 is the pre-impact velocity of car 2 in m/s

V_3 is the post-impact velocity of car 1 in m/s

V_4 is the post-impact velocity of car 2 in m/s

In the present study, the right-hand coordinate system will be used. Figure 2.9 shows the coordinate system and the angles of the two cars in the pre-impact situation. Figure 2.10 shows the angles in the post-impact situation.

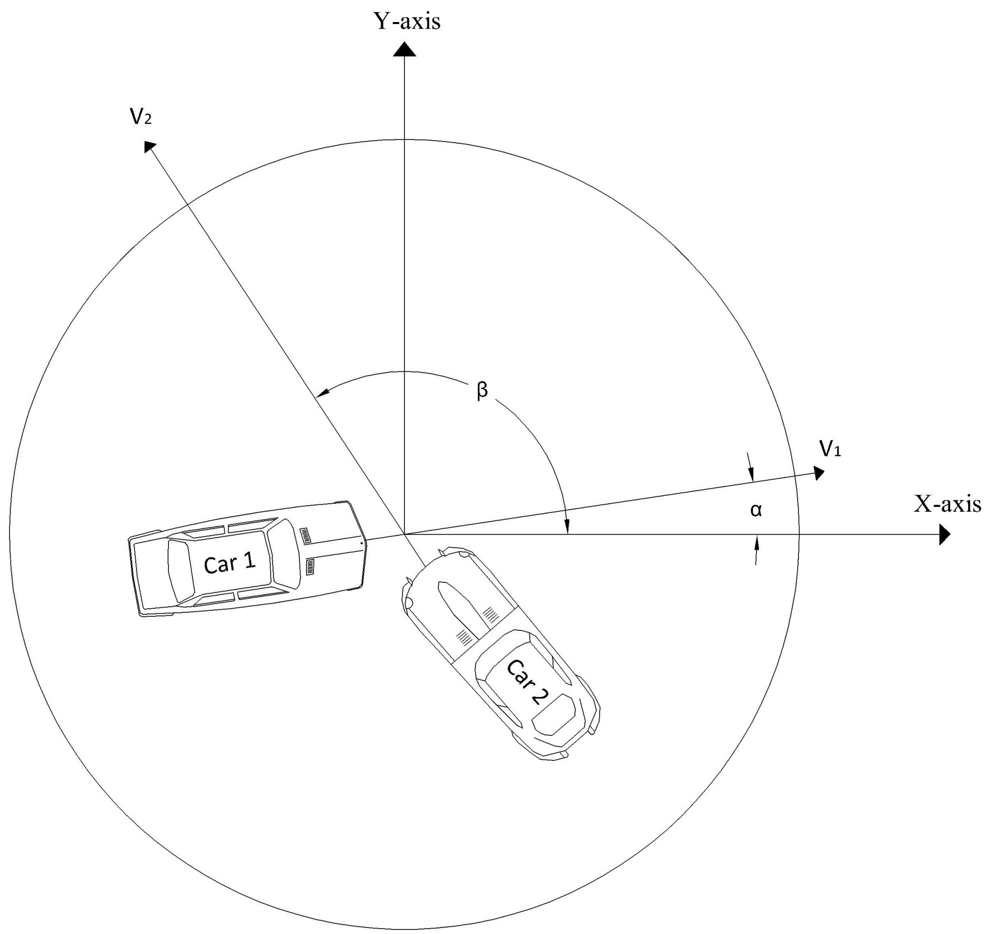

Figure 2.9: Right-hand coordinate system, pre-impact

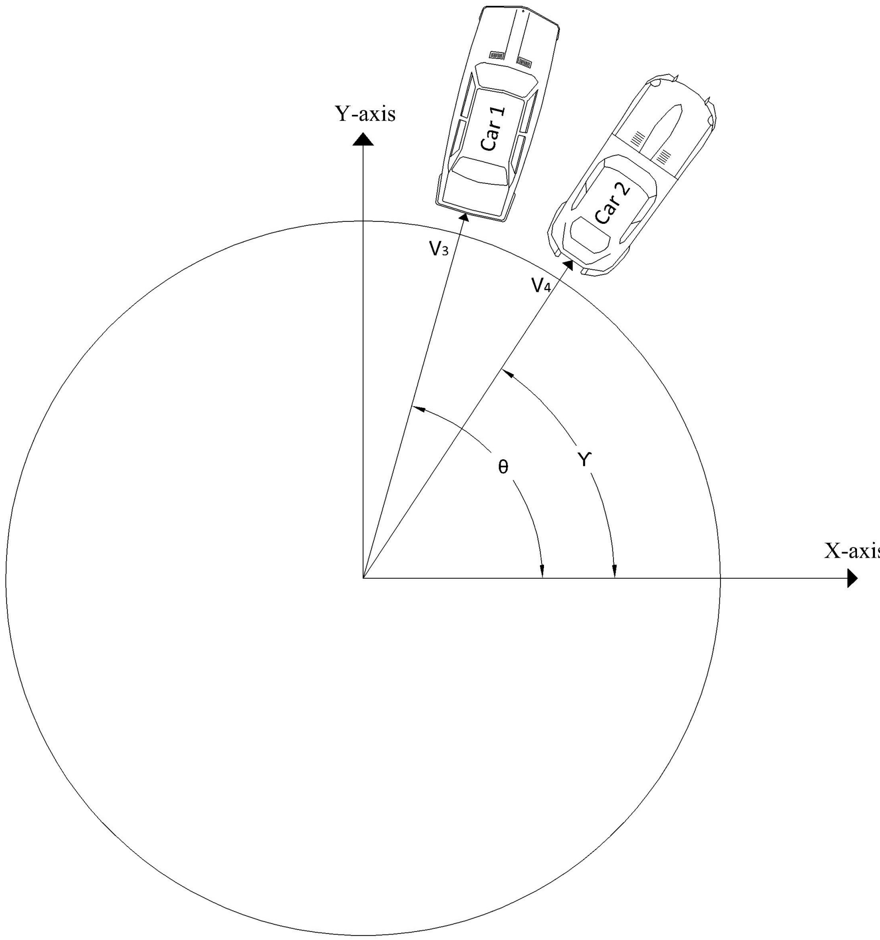

Figure 2.10: Right-hand coordinate system, post-impact

Where

α is car 1 approach angle

β is car 2 approach angle

θ is car 1 departure angle

γ is car 2 departure angle

For making equation 2.13 easier to use, it could be divided on the standard x , y and z axis, as shown in equation 2.14 below.

$$m_1V_1\ cos\lambda_1\ cos\alpha + m_2V_2\ cos\lambda_2\ cos\beta = m_1V_3\ cos\lambda_3\ cos\theta + m_2V_4\ cos\lambda_4\ cos\gamma \tag{2.14a}$$

$$m_1V_1\ cos\lambda_1\ sin\alpha + m_2V_2\ cos\lambda_2\ sin\beta = m_1V_3\ cos\lambda_3\ sin\theta + m_2V_4\ cos\lambda_4\ sin\gamma \tag{2.14b}$$

$$m_1V_1\ sin\lambda_1 + m_2V_2\ sin\lambda_2 = m_1V_3\ sin\lambda_3 + m_2V_4\ sin\lambda_4 \tag{2.14c}$$

Where λ_1, λ_2, λ_3 and λ_4 are the angles between the heading of the vehicles and the road for V_1, V_2, V_3, and V_4 respectively, as shown in figure 2.11, where the x-y plane is the road plane.

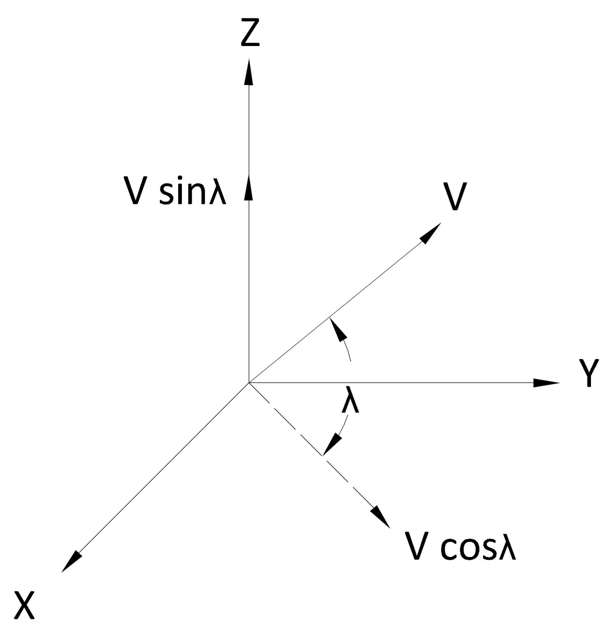

Figure 2.11: Road grade angle

In addition, the change in velocity for each car could be found using equation 2.15, as shown below.

$$\Delta V_1 = \sqrt{V_1^2 + V_3^2 - 2V_1V_3 \, cos\theta} \tag{2.15a}$$

$$\Delta V_2 = \sqrt{V_2^2 + V_4^2 - 2V_2V_4 \, cos\gamma} \tag{2.15b}$$

As it was defined, the momentum is a vector quantity, and it has the same direction of the velocity acting on the car. So the direction of action acting on the change of momentum, and usually this is the direction of the damage side, called the Principal Direction of Force (PDOF), see figure 2.12. It can be calculated using equation 2.16.

$$PDOF_1 = sin^{-1}\left(\frac{V_3 \, sin\theta}{\Delta V_1}\right) \tag{2.16a}$$

$$PDOF_2 = sin^{-1}\left(\frac{V_4 \, sin\gamma}{\Delta V_2}\right) \tag{2.16b}$$

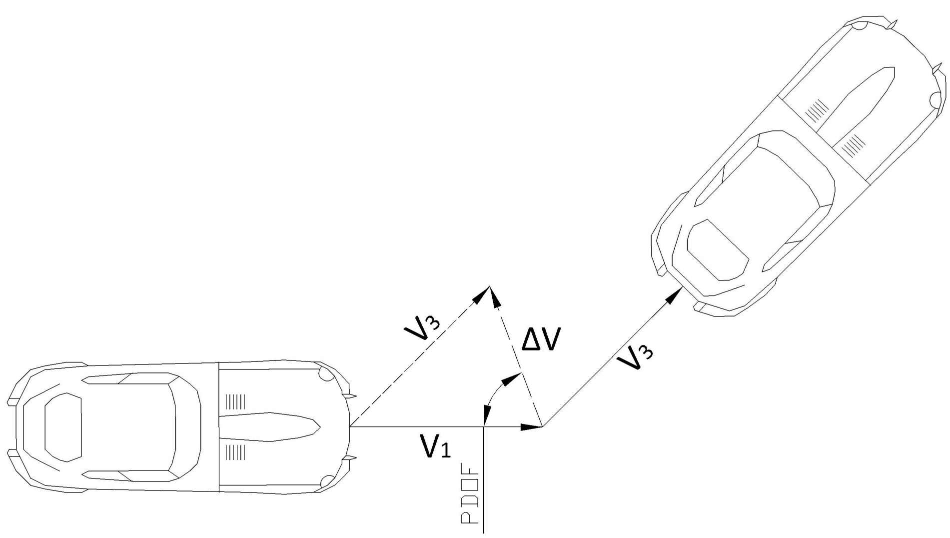

Figure 2.12: PDOF angle

2.4 Conservation of Energy in car accident collision

The conservation of energy indicates that the total energy of an isolated system remains constant, energy can be neither created nor be destroyed, but it transforms from one form to another and its SI unit is $(Joules = Nm)$[5].

In particular accidents where no enough information is available about the two moving cars speeds (for example no skid marks), the principal of conservation of energy could be combined with the principal of conservation of linear momentum to predict the speeds of the cars in the accident (pre and post-impact speeds).

Taking one car in an accident, the total energy of the car before the impact equals the energy after the impact (the summation of the energy that deformed the body of the car and the energy that moves the car after the collision), as shown in equation 2.17. Notice that the closed system in this study is the instantaneous velocity before and after the collision, so the potential energy in these equations will equals zero.

$$KE_{before} = KE_{after} + E_{deformation} \tag{2.17}$$

Where

KE_{before} is the kinetic energy before the impact

KE_{after} is the kinetic energy after the impact

$E_{deformation}$ is the energy consumed in the deformation

And the kinetic energy could be calculated using equation 2.18.

$$KE = \frac{1}{2}mV^2 \tag{2.18}$$

By rearranging equation 2.17 and 2.18 for the two cars as it was specified for the velocities labels in the previous sections to reach equation 2.19.

$$\frac{1}{2}m_1V_1^2 = \frac{1}{2}m_1V_3^2 + E_{deformation\ 1} \tag{2.19a}$$

$$\frac{1}{2}m_2V_2^2 = \frac{1}{2}m_2V_4^2 + E_{deformation\ 2} \tag{2.19b}$$

Where

m_1 is the mass of car 1 in Kg

m_2 is the mass of car 2 in Kg

V_1 is the pre-impact velocity of car 1 in m/s

V_2 is the pre-impact velocity of car 2 in m/s

V_3 is the post-impact velocity of car 1 in m/s

V_4 is the post-impact velocity of car 2 in m/s

$E_{deformation\ 1}$ is the energy deforms car 1 in Nm

$E_{deformation\ 2}$ is the energy deforms car 2 in Nm

After a collision deforms the car body, a profile of the damaged area could be drawn based on the original profile of the car, the difference between the pre and post impact car profile is defined as the Damage Profile. By using the damage profile of the crashed car, equation 2.20 could be found[6].

$$E_{deformation} = \int_0^L \int_0^C F\ dx\ ds \tag{2.20}$$

Where

F is the force acting between the two cars

L is the length of the damaged area

C is the depth of the damaged area, usually the average of six depth used to be measured see figure 2.13.

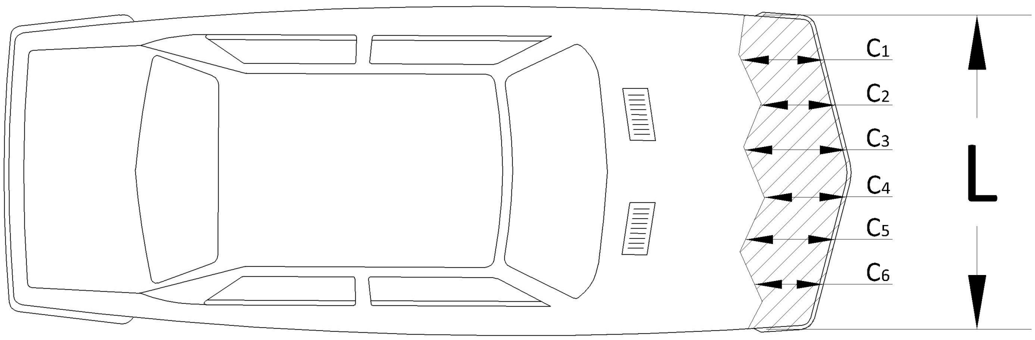

Figure 2.13: Damage profile

By solving equation 2.20 finally to reach equation 2.21 as shown[6].

$$E_{deformation} = \frac{L}{5}\Bigg(\frac{A}{2}\Big(C_1 + 2C_2 + 2C_3 + 2C_4 + 2C_5 + C_6\Big) + \frac{B}{6}\Big(C_1^2 + 2C_2^2 + 2C_3^2 + 2C_4^2 + 2C_5^2 + C_6^2 + C_1C_2 + C_2C_3 + C_3C_4 + C_4C_5 + C_5C_6\Big) + \frac{5A^2}{2B}\Bigg) \tag{2.21}$$

Where

A is the stiffness coefficient before permanent damage in N/m

B is the stiffness coefficient per meter depth and width in N/m^2

L is the length of the damage area in m

C_1 *to* C_6 are six measurements of the damage depth along the length L in m

Also the stiffness coefficient A represents the maximum force per unit width of the contact area which produce no deformation, and the stiffness coefficient B represents the ratio of the force per unit width of the contact area to the deformation depth. It is important to notice that these coefficients are calculated based on the crash tests data[6]. Many simulation software used in car accident reconstruction provides a database of the stiffness coefficients, for example the stiffness coefficients of some cars are provided in table 2.1 as given in ARAS simulation software[7].

Table 2.1: Car stiffness coefficients

Car	**Stiffness coefficients**	
(maker-year-model)	**A** (N/m)	**B** (N/m^2)
Volkswagen - 2013 - Tiguan	175244.6	3144280
Dodge - 2007 - Charger	86499	701170
Ford - 1999 - Explorer	653196.1	31896620

Finally by substitution of $E_{deformation}$ (equation 2.21) in the conservation of energy (equation 2.19), the obtained equations could be combined with the equations of linear momentum (equation 2.14) to solve for the four unknown variables (V_1, V_2, V_3, V_4).

2.5 Injuries

In some cases the investigator couldn't find a logical injury for one of the passengers or the pedestrian, the Department of Transport in London made statistics and studies to estimate relationship between speed and risk of fatal injury. Figure 2.14 shows the relation between impact speed and fatal risk for a pedestrian, and figure 2.15 and 2.16 shows the relation between ΔV and the fatal risk for the driver in frontal impact and side impact with another vehicle respectively.

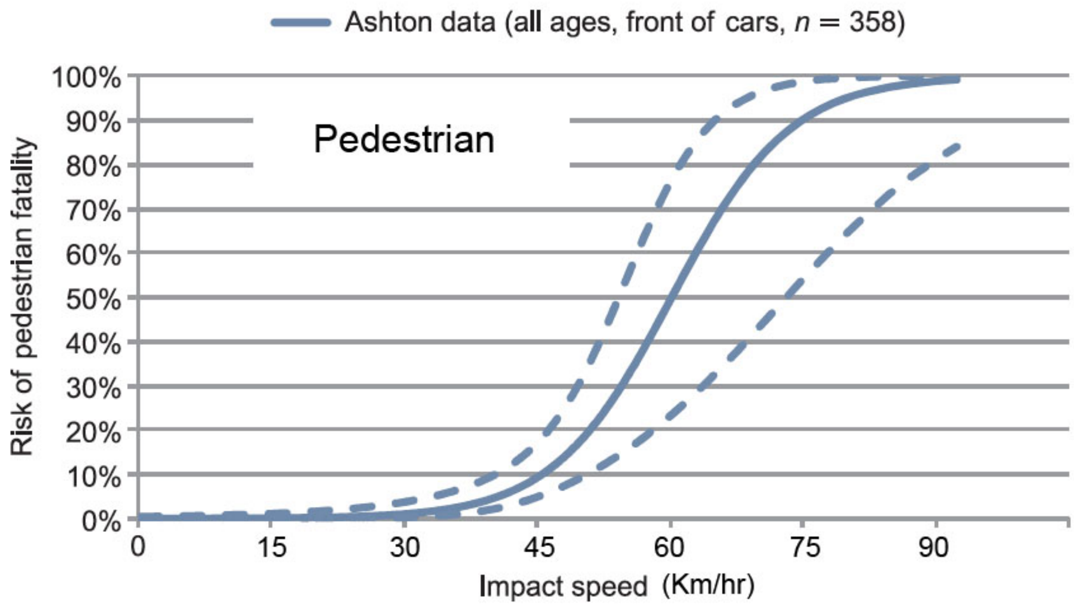

Figure 2.14: Relation between impact speed and risk of injury for a pedestrian[8]

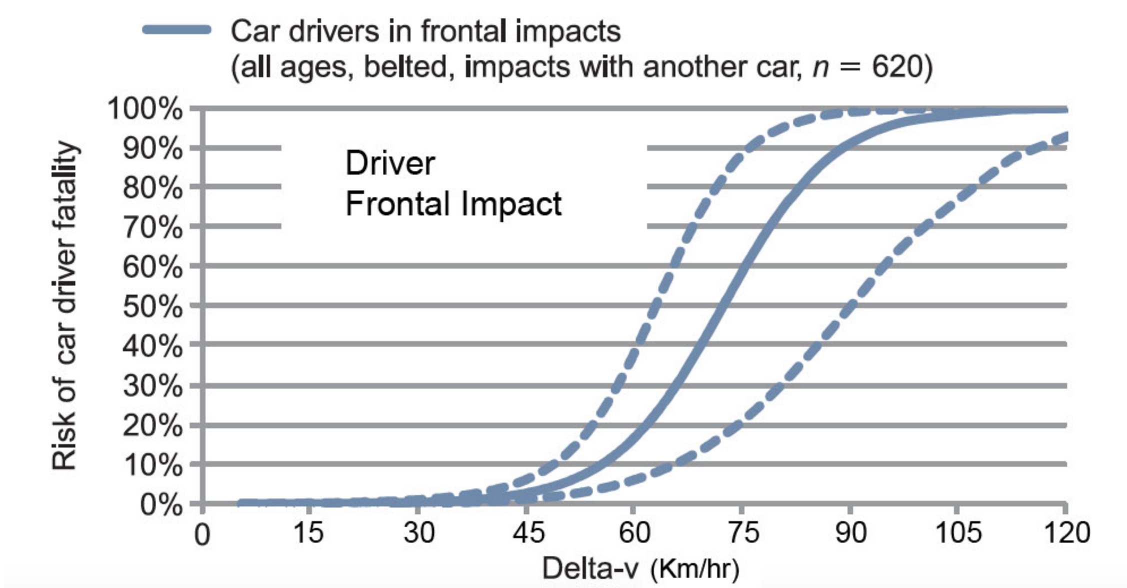

Figure 2.15: Relation between ΔV and risk of injury for a driver in frontal accident[8]

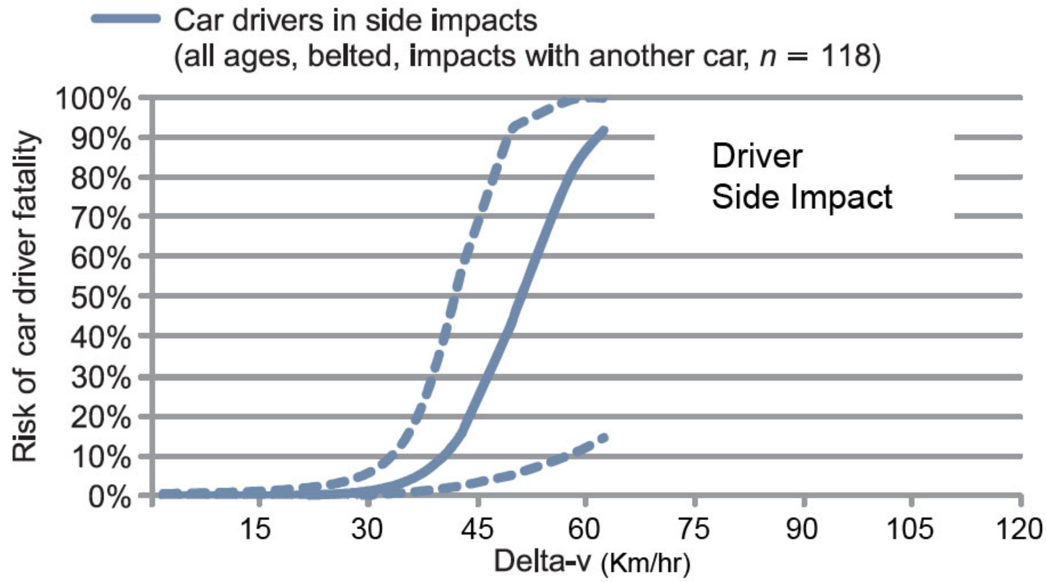

Figure 2.16: Relation between ΔV and risk of injury for a driver in side accident[8]

CHAPTER 3

ROLE OF TIRE MARKS IN CAR ACCIDENT INVESTIGATIONS

3.1 Introduction
3.2 skid marks
3.3 Yaw striations

Chapter 3

Role of tire marks in car accident investigations

3.1 Introduction

In some cases Conservation of Linear Momentum needs additional data from accident site to be solved, so we need additional information to assist linear momentum. One of the information that can be collected from the accident site is the tire marks, which provide us with useful information such as stopping distance. A tire mark is the visible mark left by tires on roads occur when a car wheel stops rolling and slides or spins on the surface of the road, see figure 3.1. Tire marks could happen due to braking only, or due to steering and Yaw striations, or both together, which will be discussed in the present chapter. Tire marks can be analyzed to predict car speed prior to an accident[9].

Figure 3.1: Tire marks

Talking about tire marks and braking leads to a very important terminology, which is the Stopping Distance, it is the distance between the moment when hazard is recognized and the moment when the car comes to a complete stop. In other words, it is the sum of the distance traveled during the reaction time, and the braking time[10]. Where the reaction time is the period between recognizing the hazard and decision to brake, and the time it takes the foot to hit the brake pedal. It ranges between 0.3 to 1.7 seconds depending upon the driver[11]. And braking time defined as the period between pressing on the brake pedal until the car comes to a complete stop[10]. See figure 3.2.

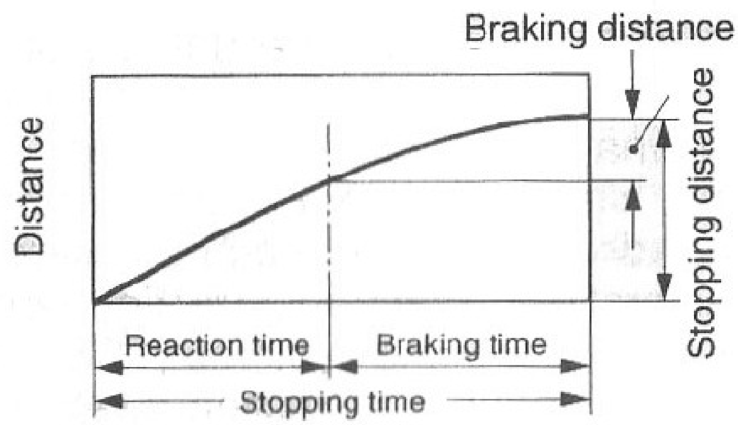

Figure 3.2: Stopping distance

Stopping distance is a directly proportional relation with car speed. In figure 3.3 an average family car used to make this graph, with the following assumptions[12]:

1) Reaction time of 1.5 second

2) A modern car with good brakes and tires

3) A dry road that is sealed and level has a coefficient of friction of approximately 1

4) A wet road that is sealed and level has a coefficient of friction of approximately 0.7

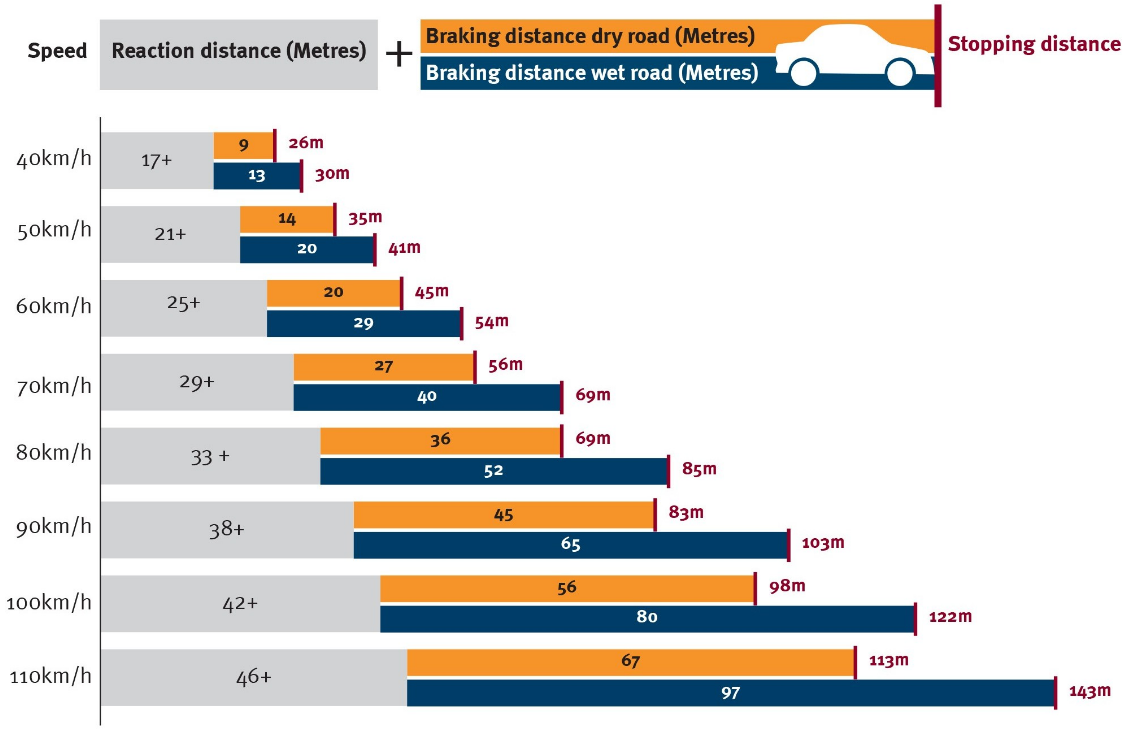

Figure 3.3: Stopping distance in different speeds[12]

There are some factors affecting the stopping distance, here some of them[12]:

1) **Driver factors:**

- Attention
- Fatigue
- Impairment due to alcohol and drugs
- Vision issues
- Driver age and experience
- Hazard perception ability

2) **Vehicle factors:**

- Vehicle age

- Type and condition of brakes
- Type and condition of tyres, including tyre pressure
- Safety features fitted to the vehicle (e.g. ABS, ESC, EBA, etc.)
- Vehicle weight
- Towing a trailer or carrying a heavy load

3) **Environmental factors:**

- Road surface
- Road gradient
- Road alignment
- Weather conditions

3.2 skid marks

As it was mentioned before, skid mark is one of the tire marks types. Skid mark defined as the tire mark on the road surface produced by a tire that is locked[9]. The skid mark usually appears light at the first, then it goes darker, and if the car stops without crash with any thing, the skid mark finish with a sharp end.

To predict and calculate the minimum speed from the skid mark, mainly there are three factors affecting on:

1) Skid distance

2) The drag factor for the road surface

3) Car braking efficiency

3.2.1 Skid Distance

Skid mark speed is the speed of the car at the beginning of the skid mark, which means at the moment the driver press on the brake pedal. When the wheels start to slow just before they full lock, there will be a light mark produced. The shadow mark and the clearly visible mark for the same tire must be continuous. Modern brake systems lock the four wheels at the same time, and if the car is going in a straight line, the rear wheels skid marks will overlap the front wheels skid marks. In this case front wheels skid marks could be identified by the lighter mark during the total mark, and the rear wheels skid marks identified by the darker mark in the center of the total mark. See figure 3.4.

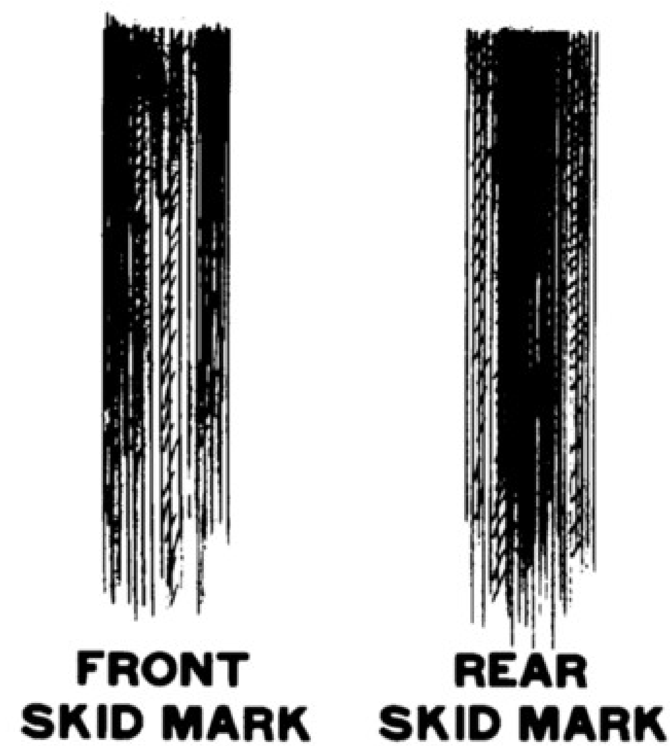

Figure 3.4: Front-rear skid mark

In other cases the four skid mark can be found, so here the four marks should be measured to calculate the average of them. If the rear wheels skid marks overlap the front wheels marks, the total skid marks we get must be measured. The average skid distance can be found using equation 3.1 shown below.

$$D = \frac{k_1 + k_2 - (0.5)L}{2} \tag{3.1}$$

Where

D is the average skid distance

k_1 is the first skid mark

k_2 is the second skid mark

L is the wheelbase (distance between front and rear tires)

3.2.2 Drag Factor

A drag factor is the term for the tire-road surface interface when determining car speeds[9], and it found experimentally. Table 3.1 shows the most popular road conditions and their drag factor.

Table 3.1: Drag factor with different road conditions[9]

Road condition	Drag factor
Portland Cement	0.55 - 1.20
Asphalt	0.50 - 0.90
Gravel	0.40 - 0.80
Ice	0.10 - 0.25
Snow	0.10 - 0.55

Also drag factor could be calculated from the accident site for more accurate result to include the road and tire conditions. For this test the tire of the vehicle and a spring balance is needed on the accident site, the spring should be attached to the tire and pulled in a constant speed to calculate the static coefficient of friction (Drag factor), as shown in equation 3.2.

$$f = \frac{F_s - mgsin(\lambda)}{mgcos(\lambda)} \tag{3.2}$$

Where

f is the drag factor

F_s is the force read from the spring balance in newton

m is the mass of the tire in Kg

g is the standard of gravity which equals 9.81 m/s^2

λ is the road angle, see figure 2.11

3.2.3 Braking efficiency

Each wheel on a car provide a certain amount of the total brake force available. Which means that each wheel has a percentage of the total brake force, which called braking efficiency, as shown in table 3.2 below[9].

Table 3.2: Braking efficiency

Brake condition	Braking efficiency
Front wheels braking only	60%
Rear wheels braking only	40%
All wheels braking	100%

Which means that each front wheel has a 30% braking efficiency, and each rear wheel has a 20% braking efficiency.

Form the previous three variables (skid distance, drag factor and braking efficiency), the minimum skid speed can be found using the empirical equation 3.3 as shown below.

$$S_k = \sqrt{(254 \cdot D \cdot f \cdot n \cdot cos(\lambda)) + (254 \cdot D \cdot sin(\lambda))} \tag{3.3}$$

Where

S_k is the minimum skid speed in km/h

D is the average skid distance in meters

f is the drag factor

n is the braking efficiency

λ is the road angle

It is important to notice that this equation assume that the car still skidding until its speed reach to zero, but if there a crash happens, the residual speed value must be combined with the calculated minimum skid speed, as shown in equation 3.4.

$$S_c = \sqrt{S_i^2 + S_k^2} \tag{3.4}$$

Where

S_c is the combined car speed

S_i is the pre-impact car speed

S_k is the calculated minimum skid speed

Finally, for a car with Anti-locking Brakes system on the four wheels, deduct 10% from the calculated skid speed from equation 3.3 [9]. Figure 3.5 shows the difference between locked and anti-locked wheels brake skid marks.

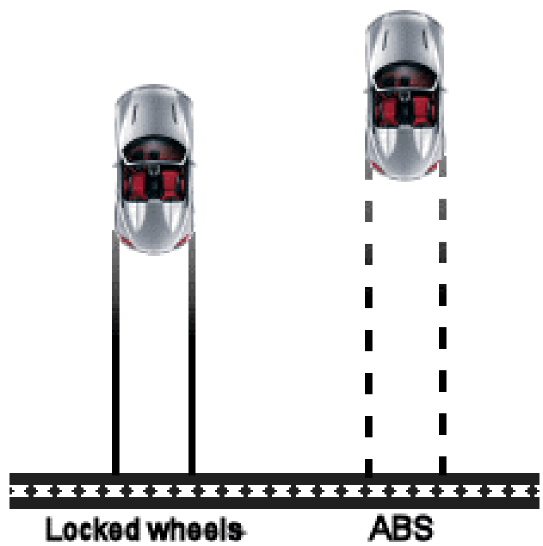

Figure 3.5: Locked and anti-lock braking skid mark

3.3 Yaw striations

It is important to determine the braking and steering situation before the impact, which could help the investigator to predict the cause of the accident. In the present section the concept of determining car steering and braking from Yaw striations will be discussed.

Yaw striations are one of the tire marks, it happens when the car is traveling into a curve by steering only or steering with braking together. Figure 3.6 shows the difference between Yaw striations with no braking and with full braking and the transition zone. The no braking striations usually inclined at an angle from the direction of travel.

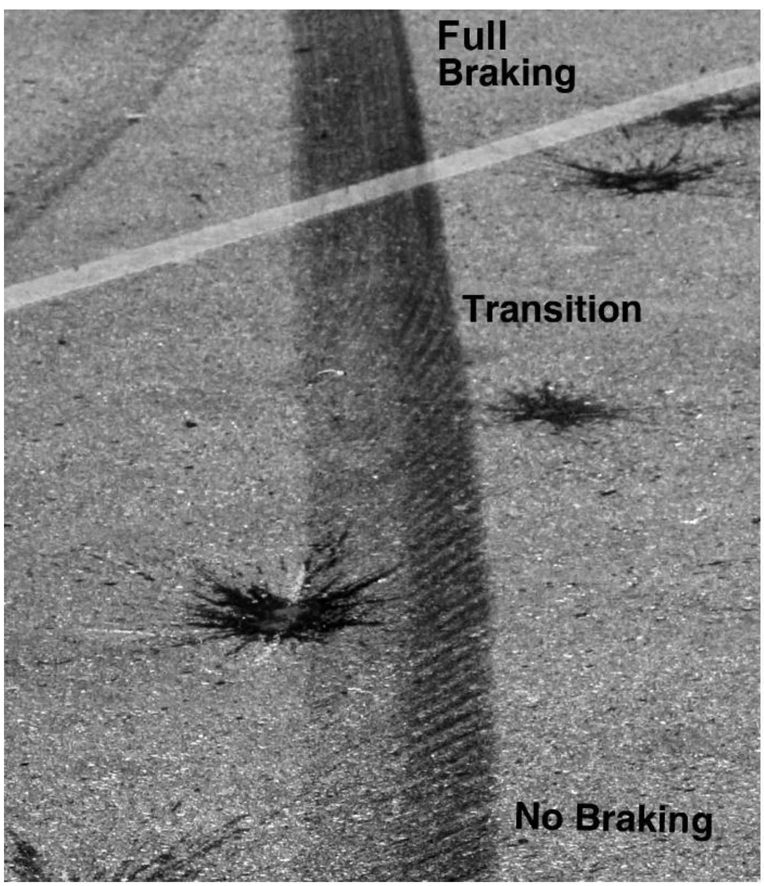

Figure 3.6: Yaw striations in different situations

Some new terminology are going to be used in this section (such as direction of heading, direction of travel and slip angle). The direction of heading defined as the direction of the steering or the desired steering angle from the driver. On the other hand, the direction of travel defined as the direction which the car directs to due to tire slip. Finally the slip angle defined as the angle between the direction of heading and the direction of travel[13]. Notice that if there is no tire slip the direction of travel will be the same as the direction of heading, see figure 3.7, where ϕ is the slip angle, the gray lines are the patch contact striations and the black lines are the shoulder striations.

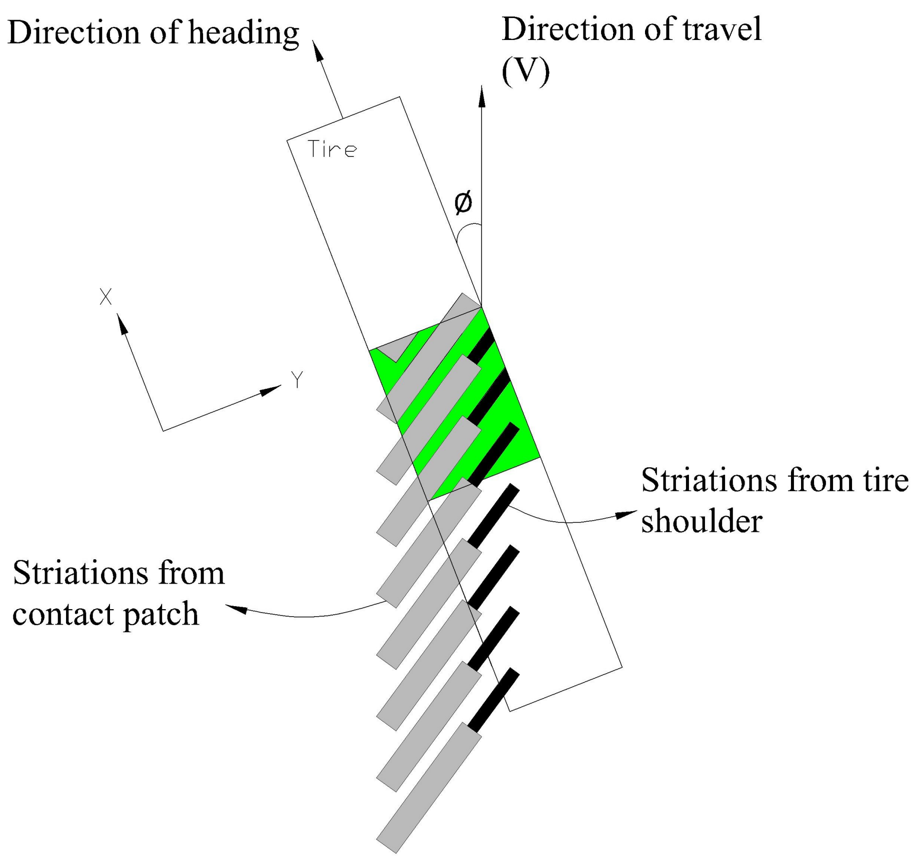

Figure 3.7: Direction of heading/travel and slip angle

Usually the tire contacts the road surface in a space called patch contact as seen in figure 3.7 by the green zone, but in some cases the tire shoulder(the portion of the tread between the tread center and the tire sidewall) make striation as shown in figure 3.8.

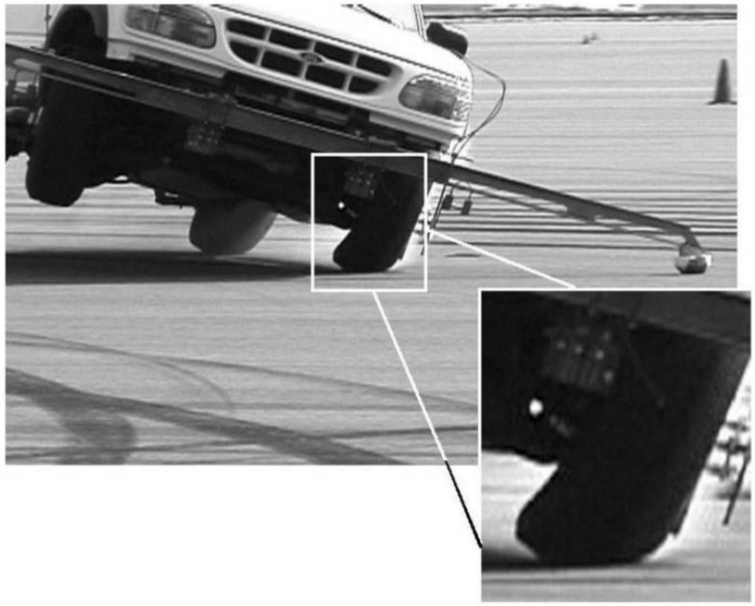

Figure 3.8: Tire shoulder contacts the road surface

Notice that when the car under steering only the striations are perpendicular to the direction of heading, and when the car under full braking the striations are parallel to the direction of travel, see figure 3.6.

3.3.1 Determining car steering form Yaw striations

At the first it is important to pay attention that in the present project the tire will be assumed as a rigid body. As it was mentioned ϕ is the slip angle between the direction of heading and the direction of travel or the velocity, also δ could be the angle between the direction of travel and the direction of striations, finally the summation of $(\phi + \delta)$ will be Ψ which is the angle between the direction of heading and the direction of striations[13], as shown in figure 3.9.

Moreover, the Contact Patch Length (CPL) is defined as the length of the contact patch, and the distance between the striations measured along the velocity direction is defined as the Striation Distance (SD), also the spacing between the tread blocks on the tire defined as the Tread Distance (TD), see figure 3.9.

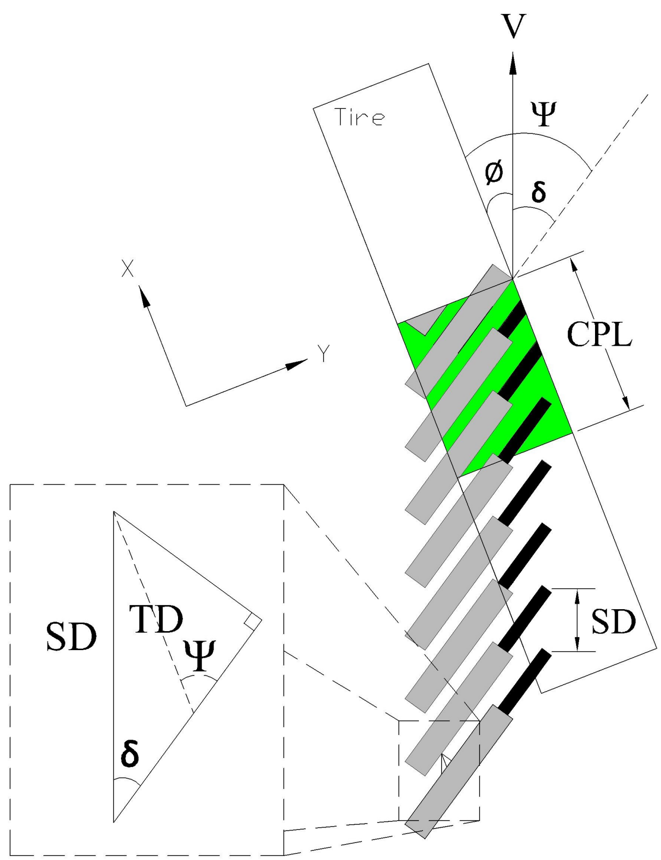

Figure 3.9: Top view of Yawing angles

By analysis of the two triangles on the left lower corner of figure 3.9, equation 3.5 could be found as follows[13].

$$\Psi = sin^{-1}\left(\frac{SD\ sin\ \delta}{TD}\right) \tag{3.5}$$

It was defined that

$$\Psi = \phi + \delta \tag{3.6}$$

By rearrange equations 3.5 and 3.6 to reach equation 3.7 as shown below.

$$\phi = sin^{-1}\left(\frac{SD\ sin\ \delta}{TD}\right) - \delta \tag{3.7}$$

All the variables in equation 3.7 could be measured from the accident site or the tires. From equation 3.7 the slip angle could be calculated. Slip angle (ϕ) is very useful, where it helps the investigator to predict the steering angle that the driver was aiming to based on the basics of the vehicle dynamics rules as shown in equation 3.8 below[14].

$$\varepsilon = \frac{L}{R}\, 57.3 + \phi_f - \phi_r \tag{3.8}$$

Where

ε is the steering angle by the driver

L is the wheel base of the car

R is the radius of the curve the car is Yawing into

ϕ_f is the front wheel slip angle

ϕ_r is the rear wheel slip angle

3.3.2 Determining car braking form Yaw striations

Determining the braking situation (braking slip percentage) is very important, because in some cases it could be calculated when the slip angle could not. Braking slip is defined by the ratio of slip velocity in the contact patch (forward velocity (V) - tire circumferential speed (ω)) to forward velocity[14], as shown in equation 3.9 below.

$$Slip_B = \frac{V - \omega r}{V} \tag{3.9}$$

Where

$Slip_B$ is the braking slip

V is the velocity of the car

ω is the rotational velocity of the tire

r is the tire radius

When the tires under no braking V will equal ωr and in this case the braking slip will be 0. On the other hand, when the tires under full braking ω will be 0 and the braking slip will be 1.

Assume a tire with slip angle moving from point 1 to 2 as shown in figure 3.10. It will have a travel velocity and heading velocity V and V_h respectively. For the braking slip the heading velocity is the one needed, as shown in equation 3.10.

$$Slip_B = \frac{V_h - \omega r}{V_h} \qquad (3.10)$$

By using the triangle theories we get

$$Slip_B = \frac{V cos\phi - \omega r}{V cos\phi} \qquad (3.11)$$

On the right hand of figure 3.10 shows the side view of the tire which have a radius of r and a rotational velocity ω and it is rotating a ξ in radians along the Contact Patch Length (CPL). The tire produce a Length of Striations (LS). Also the figure shows the tire mark width of w. The tire slip angle and the striation angle are shown by ϕ and δ respectively.

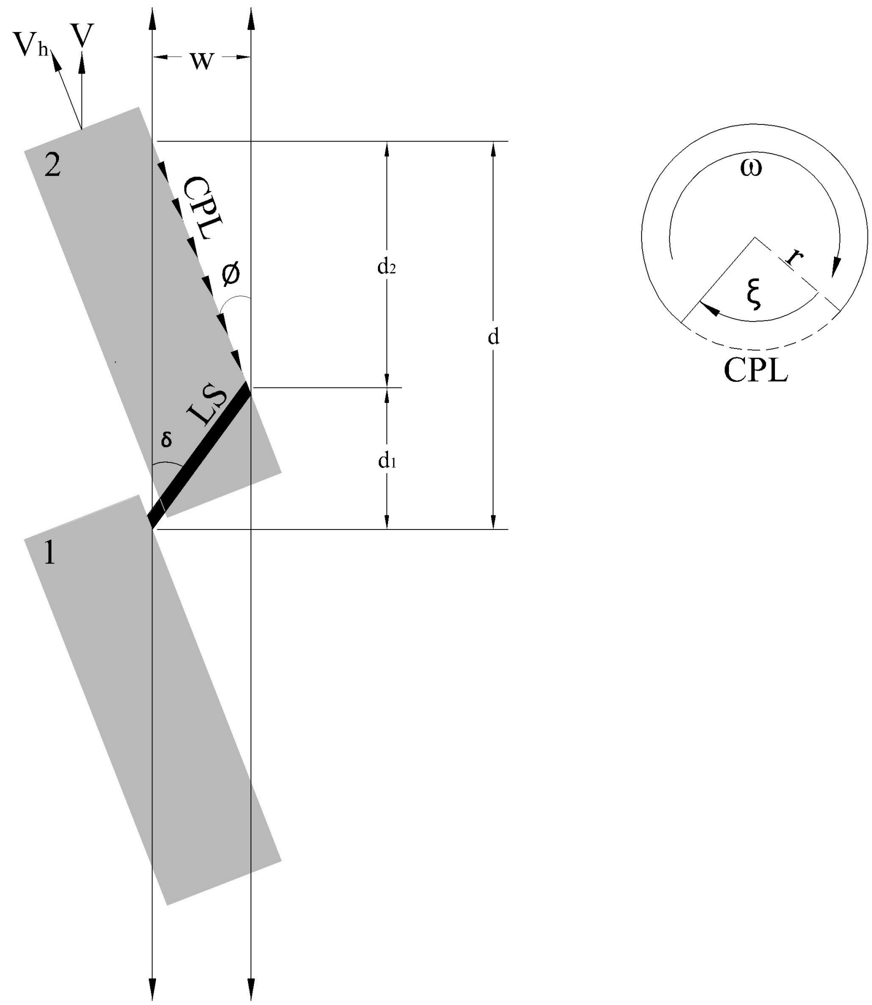

Figure 3.10: Top view of Yawing tire moving from position 1 to 2. On the right side, a side view of the tire

Also the length of striation mark measured along the direction of travel is mentioned as d_1. And the Contact Patch Length measured along the direction of travel is mentioned as d_2. and the summation of d_1 and d_2 is given as d. By rewriting equation 3.11 as a function of the time that one striation need to move to reach equation 3.12 as shown below.

$$Slip_B = \frac{\frac{d}{t}\, cos\phi - \frac{\xi r}{t}}{\frac{d}{t}\, cos\phi} \tag{3.12}$$

And by rearrange equation 3.12 we get

$$Slip_B = 1 - \frac{\xi r}{d\ cos\phi} \tag{3.13}$$

Two different triangles can be used to form two equations for the tire mark width w as shown in equation 3.14.

$$w = CPL\ sin\phi = LS\ sin\delta \tag{3.14}$$

And from the side view of the tire we find

$$CPL = \xi r \tag{3.15}$$

By rearrange equations 3.14 and 3.15 we get

$$CPL = \frac{LS\ sin\delta}{sin\phi} = \xi r \tag{3.16}$$

As it was defined before:

$$d_1 = LS\ cos\delta \tag{3.17}$$

$$d_2 = CPL\ cos\phi = \frac{LS\ sin\delta\ cos\phi}{sin\phi} \tag{3.18}$$

$$d = d_1 + d_2 = LS\ cos\delta + \frac{LS\ sin\delta\ cos\phi}{sin\phi} \tag{3.19}$$

Now by substitute equations 3.16 and 3.19 in equation 3.13 to reach equation 3.20 as shown below.

$$Slip_B = 1 - \frac{\left(\frac{LS\ sin\delta}{sin\phi}\right)}{\left(LS\ cos\delta + \frac{LS\ sin\delta\ cos\phi}{sin\phi}\right) cos\phi} \tag{3.20}$$

By simplified equation 3.20, finally to reach equation 3.21 as shown[13].

$$Slip_B\,\% = \frac{tan\phi}{tan(\delta+\phi)} * 100\% \tag{3.21}$$

Where

$Slip_B\,\%$ is the braking slip percentage

$(\delta+\phi)$ equals Ψ as it was mentioned before

Using the percentage of braking slip helps the investigator to determine whether the driver was full braking (100% braking slip) or was not braking (0% braking slip) or partially braking ($0\% <$ braking slip $< 100\%$).

CHAPTER 4

ACCIDENT RECONSTRUCTION SOFTWARE

Chapter 4

Accident Reconstruction Software

4.1 Introduction

Usually the investigator is not an engineer, so the equations obtained in chapter 2 and 3 may be hard to solve manually, in the present chapter the methods of solving the equations using computer software will be shown.

It is better to use GUI (Graphical User Interface) software to make it user friendly, the selected software was Visual Studio C# (C-sharp). But the complicated equations in the software have been solved by an internal subroutine written by Matlab.

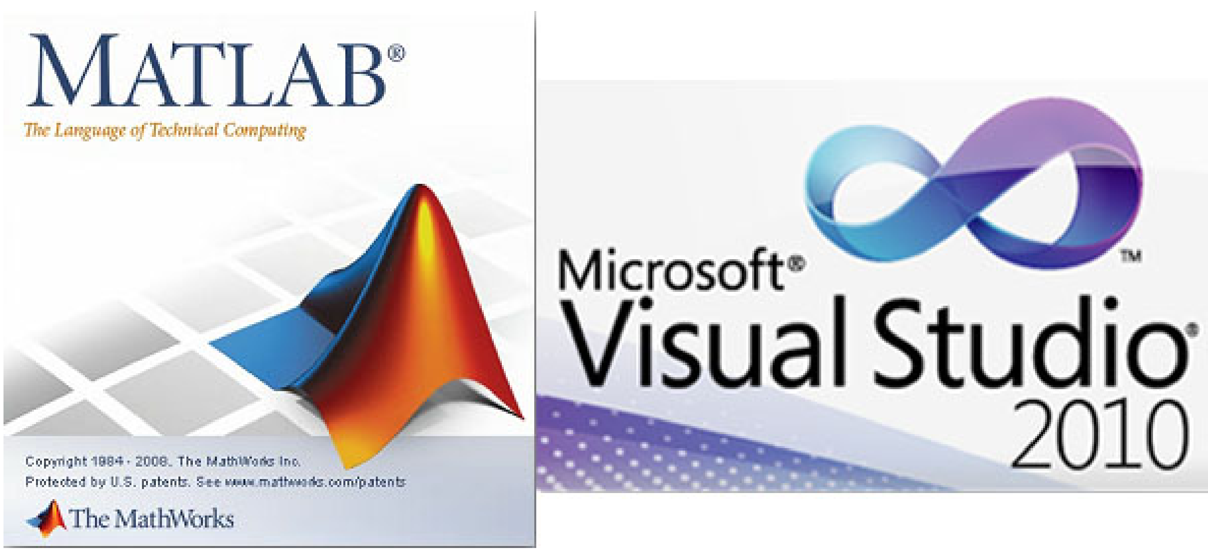

Figure 4.1: Programs Logos

4.2 Matlab

This math-work tool were used to solve four equations with four unknowns, two equations are linear and two nonlinear (Quadratic equations). These equations are the conservation of linear momentum (equation 2.14) and the conservation of energy (equation 2.19).

The Matlab code (see figure 4.2) programmed to read the inputs from a text file created by the GUI program, then this subroutine program will save the results on another text file to be read by the GUI program. So the user will just use the GUI program which is the primary program.

```
fun=@myfun;
x0=[1 1 1 1];
x=fsolve(fun,x0);
function F = myfun(x)

 [A1,A2,A3,A4,A5,A6,A7,A8,A9,A10,A11,A12,A13,A14] =textread('input.txt');
V1=x(1);
V2=x(2);
V3=x(3);
V4=x(4);
F(1)=A10*V3^2 - A9*V1^2 + A11;
F(2)=A13*V4^2 - A12*V2^2 + A14;
F(3)=A3*V3 + A4*V4 - A1*V1 - A2*V2;
F(4)=A7*V3 + A8*V4 - A5*V1 - A6*V2;

 dlmwrite('res.txt',x,'delimiter',' ');
end
```

Figure 4.2: Matlab code

Moreover, the subroutine software programmed to work in background, which means that the user will not see it. Notice that there is no need to install Matlab program on the user computer.

4.3 Visual studio C#

C-sharp program was used because it's easy enough to be self learning program, also it has many math libraries, and it's GUI is more familiar to users than other programs. Two versions were developed, a developer interface version and a user interface version.

4.3.1 Developer interface version

The complete source code with all the equations and tools are provided in this version. The reason to create a developer interface version was to allow for future modifications on the main program. The algorithm for the developer interface version was done to include all methods and tools, figure 4.3 shows the program flow diagram, and figure 4.4 shows the program algorithm diagram.

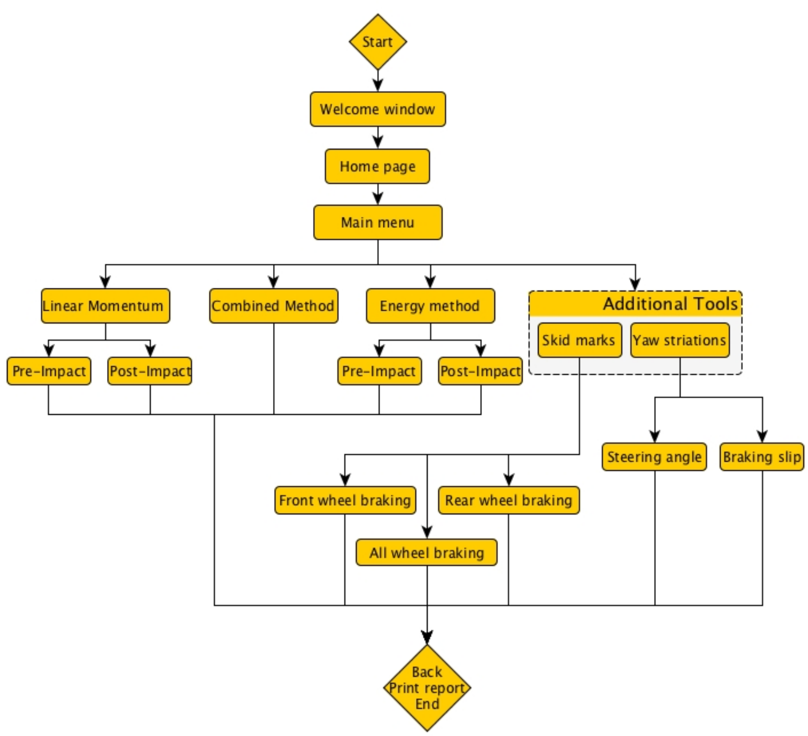

Figure 4.3: Developer interface version flow diagram

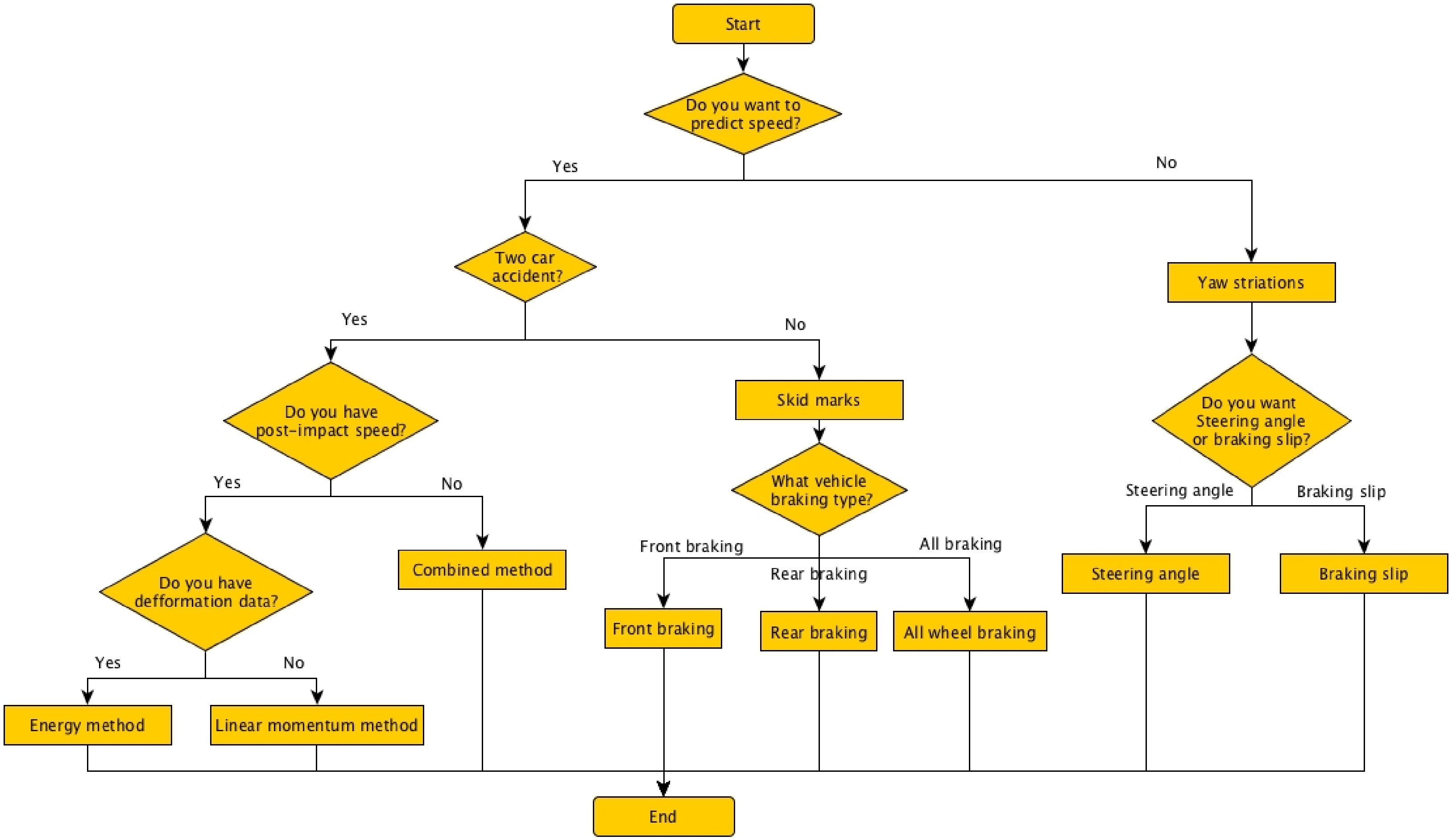

Figure 4.4: Developer interface version algorithm diagram

At the first a welcome window appear for the user, see figure 4.5.

Figure 4.5: Welcome window

The next is home page window, this request the main data for the vehicles, such as the model of each vehicle and it's weight. See figure 4.6.

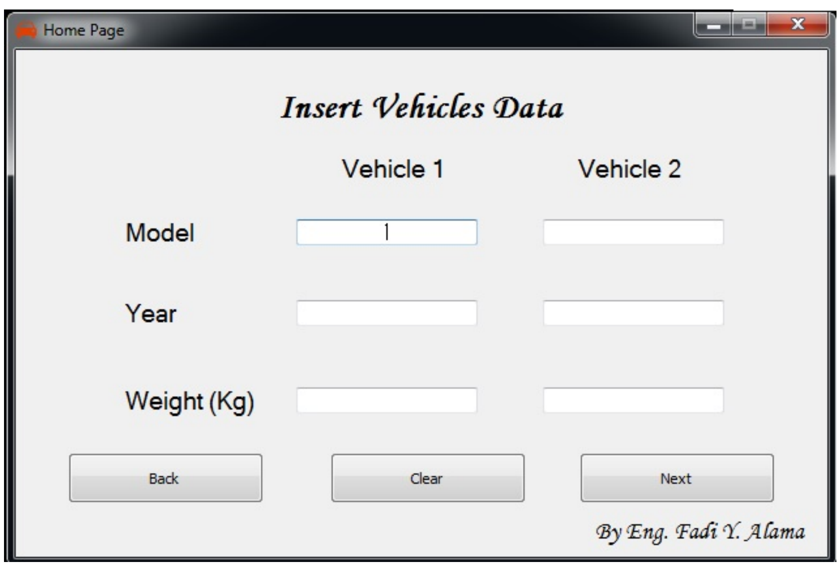

Figure 4.6: Home page window

Then the main menu will appear, this request from the user to choose a method such as (linear momentum, energy or the combined method). Also this window provide the user with the additional tools (skid marks and the Yaw striations). see figure 4.7.

Figure 4.7: Main menu window

The combined method request from the user more data about the accident such as the deformation data for each vehicle, the coefficient of stiffness for each vehicle and the angles of the vehicles. Also this window provide the user with pictures to make it easier to understand the data requested, the user can choose a picture by the buttons under the main picture, see figure 4.8. Moreover the units of each parameter were provided and a clear button was added.

Finally if the user forget to insert a parameter, an error window will alert him. Also a print report button was added to save a PDF file for a technical report including all the data and results.

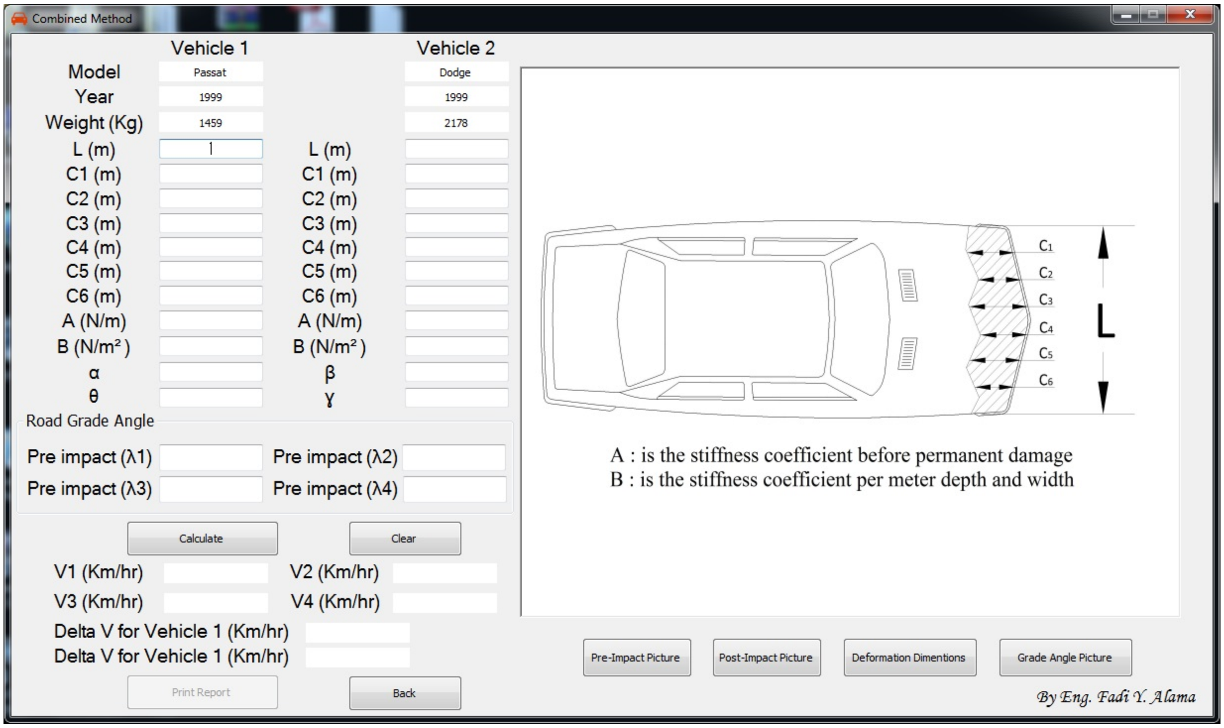

Figure 4.8: Combined method window

In the combined method shown above, the program export the data in a text file then run the subroutine program (Matlab), and wait it to finish, then the program will read the results from the new text file created by the subroutine program to complete solving the method before showing the final results for the user. Notice that the subroutine program will work in the background and the user will not be able to see it.

The linear momentum and energy methods were developed as will as the combined method, see figures 4.9 and 4.10 for the linear momentum method pre-and post-impact respectively. And figure 4.11 and 4.12 for the energy method also pre-and pos-impact respectively.

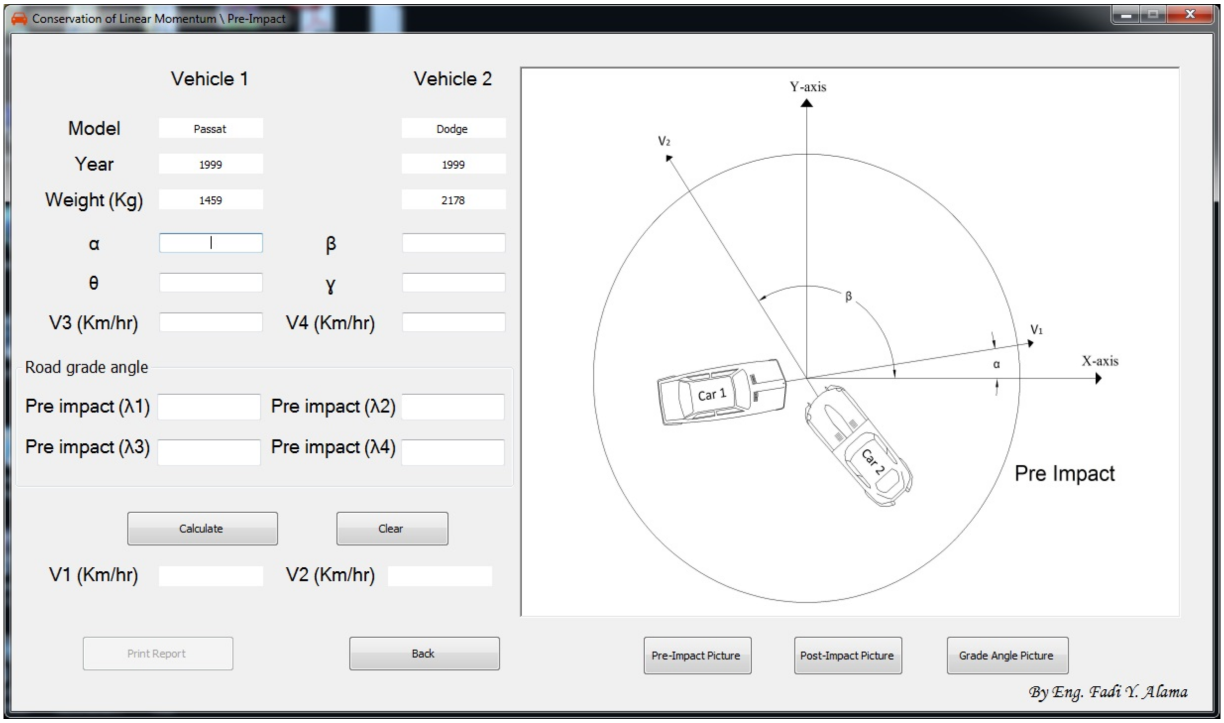

Figure 4.9: Linear momentum method/Pre-impact window

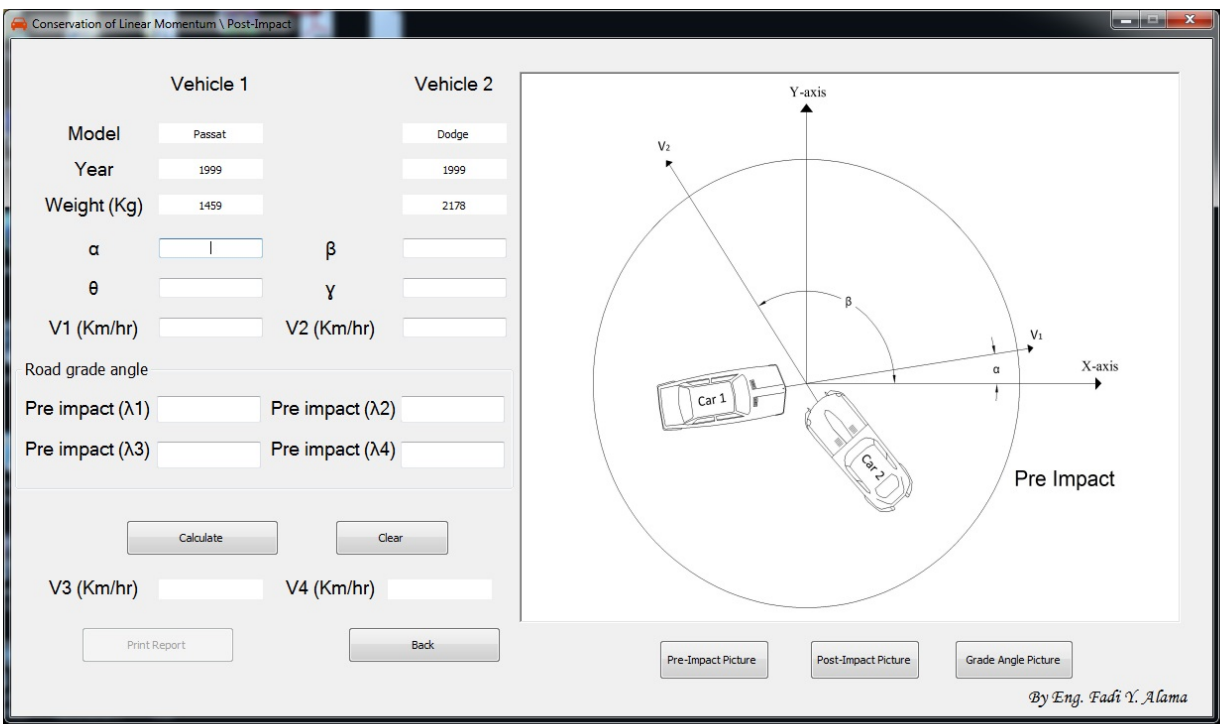

Figure 4.10: Linear momentum method/Post-impact window

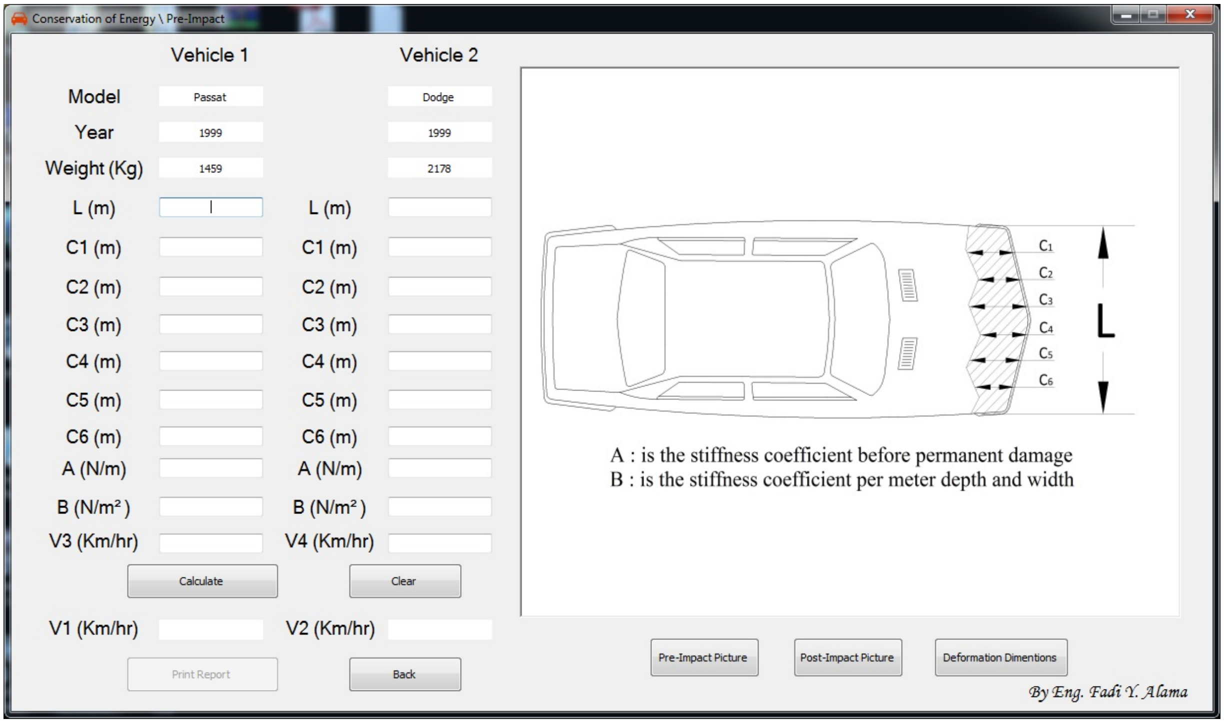

Figure 4.11: Energy method/Pre-impact window

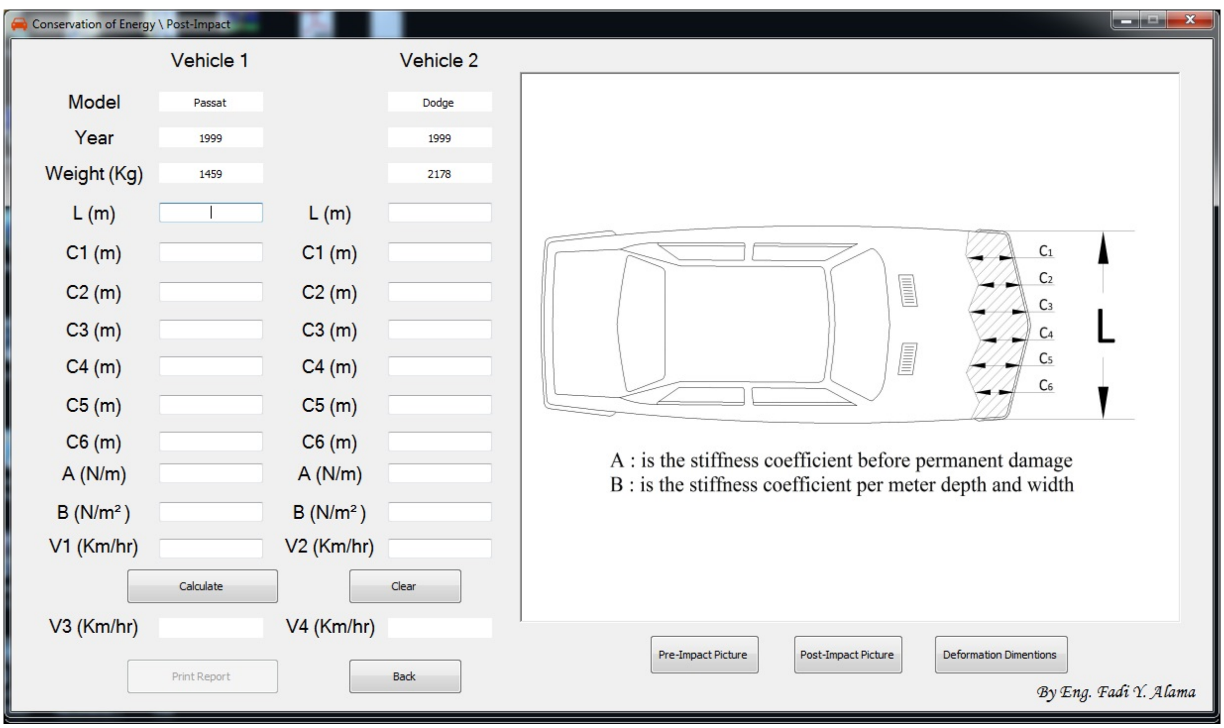

Figure 4.12: Energy method/Post-impact window

The first additional tool provided in the main menu is the skid marks, this tool ask the user about the vehicle braking type, Front, rear or all wheel braking, as shown in figure 4.13.

Figure 4.13: Skid mark window

Choosing one kind of these will give the program the braking efficiency factor, and this make it easier and faster for the user, see figure 4.14. Notice that skid mark speed calculate buttons are two, in this way the user will calculate for a vehicle With ABS and without ABS in the same window.

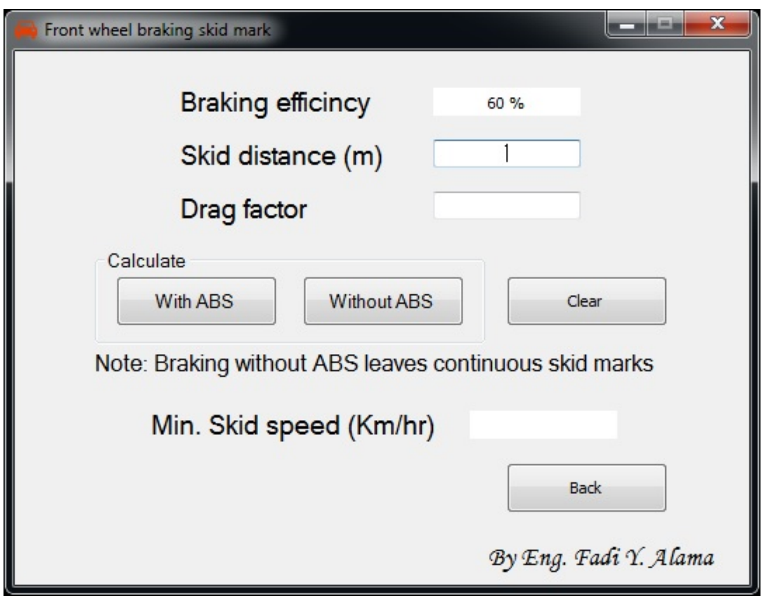

Figure 4.14: Front wheel braking skid mark window

The second additional tool provided in the main menu is the Yaw striation tool, and this tool allow the user to choose what to calculate, the steering angle or the braking slip, see figure 4.15.

Figure 4.15: Yaw striations window

For these Yaw striations tools, additional data requested from the accident site and the vehicles tires, and all of the information the user need to know are provided in the pictures in the same window such as the previous windows. See figure 4.16 and 4.17 for the steering angle and braking slip windows respectively.

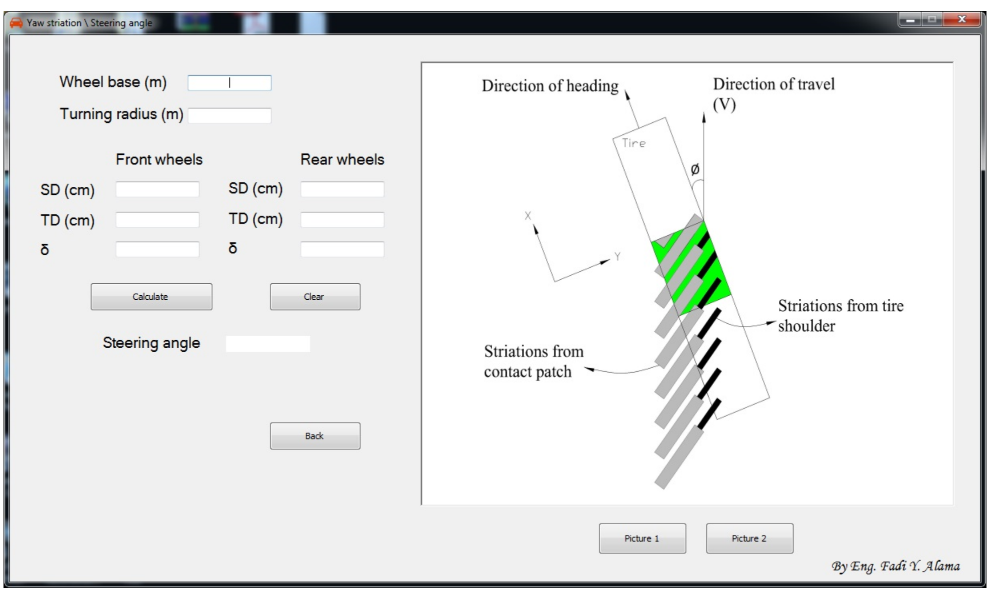

Figure 4.16: Yaw striations/Steering angle window

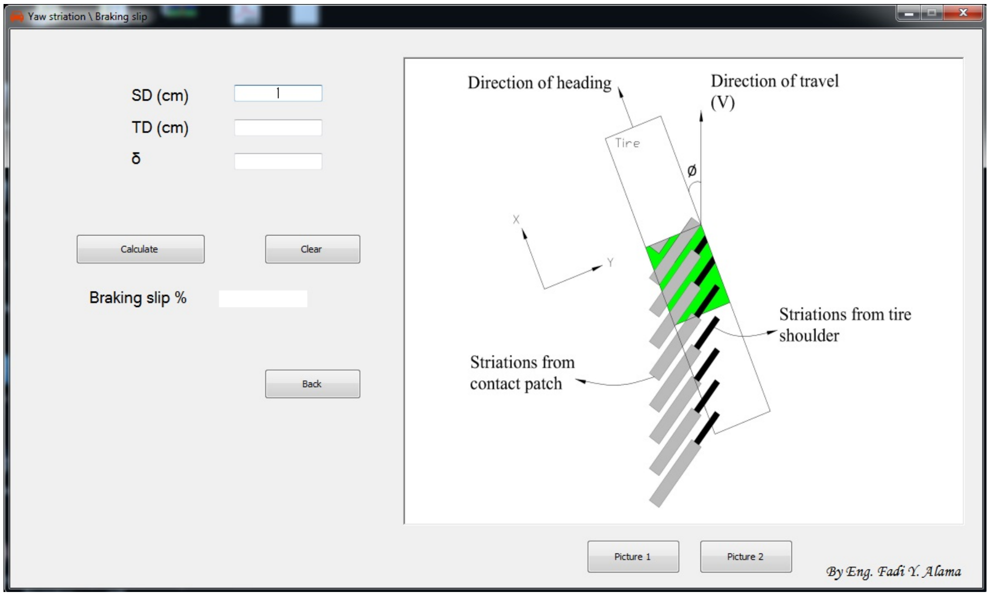

Figure 4.17: Yaw striations/Braking slip window

The technical report developed to include all the data and results for the accident, and also include some pictures to make it easier to understand the parameters. Figure 4.18 shows an example of these reports.

Palestine Polytechnic University

By : Eng. Fadi Y. Alama

Supervisor : Dr. Dyia Arafah

Combined Method

Accident Technical Report

	Vehicle 1	Vehicle 2
Model	Passat	Dodge
Year	1999	1999
Weight (Kg)	1459	2178
Pre-impact angle	310	140
Post-impact angle	100	350
Pre-Impact grade angle	1.145	-1.145
Post-Impact grade angle	-1.145	1.145
L (m)	1.4	1.85
C1 (m)	0.68	0.53
C2 (m)	0.53	0.62
C3 (m)	0.41	0.65
C4 (m)	0.3	0.64
C5 (m)	0.23	0.49
C6 (m)	0.27	0.34
Coefficient of stiffness A (N/m)	79497	68737
Coefficient of stiffness B (N/m²)	602900	787811
Pre-impact Speed (Km/hr)	50.45	67.68
Post-impact Speed (Km/hr)	19.25	28.31
Delta V (Km/hr)	57.04	40.1

Figure 4.18: Example of technical report

4.3.2 User interface version

The user interface version developed for direct use by users to analyze real accident data, such as police officers. This version include just the needed method to reconstruct car to car accident and single car accident. Figure 4.19 shows the flow diagram for this version, and figure 4.20 shows the algorithm diagram.

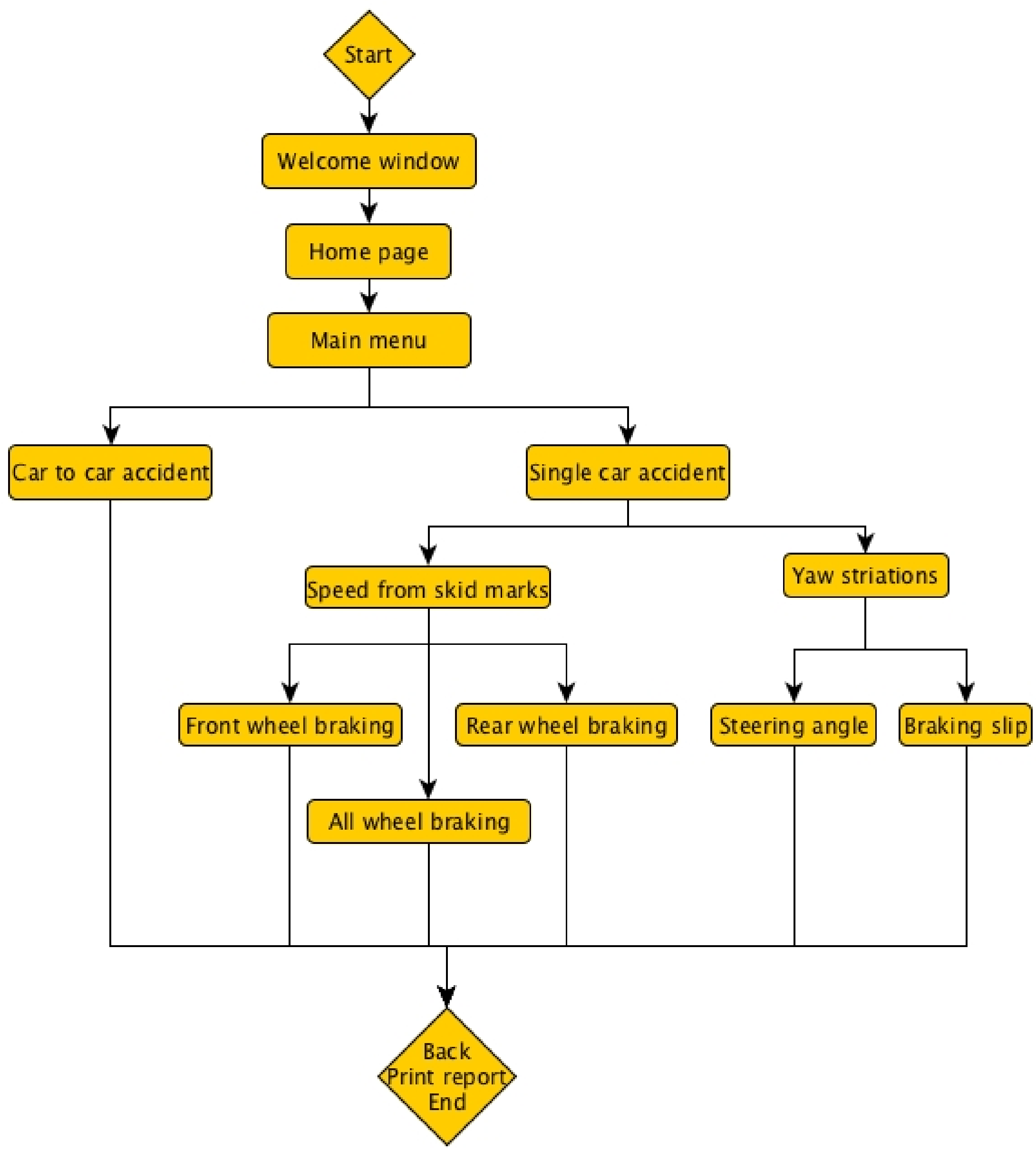

Figure 4.19: User interface version flow diagram

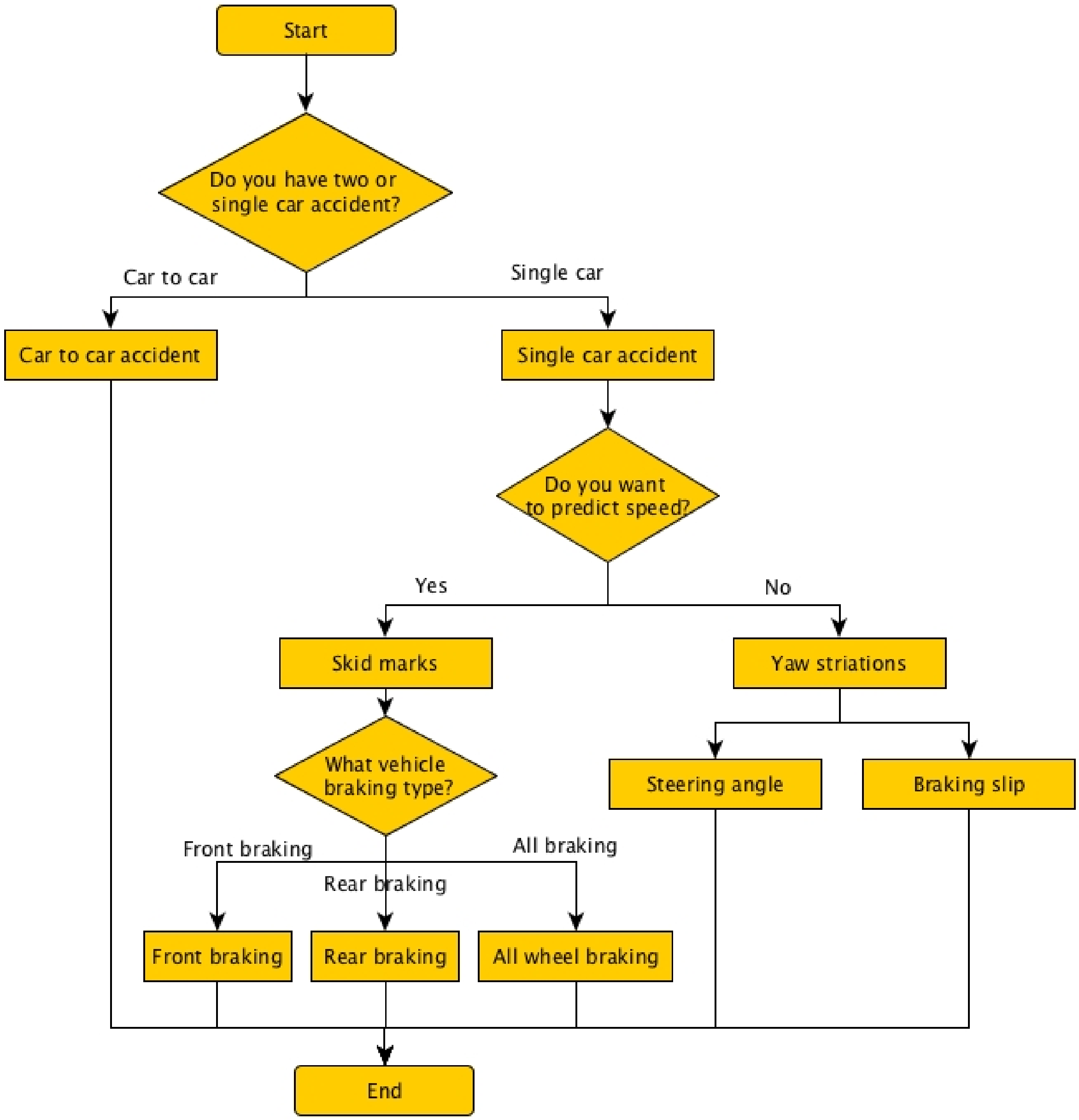

Figure 4.20: User interface version algorithm diagram

In this version the main menu developed to be easier for the user and the program ask the user about the accident type, car to car accident or single car accident, see figure 4.21.

Figure 4.21: Main menu window

Choosing the car to car accident button will move the user to the combined method directly, and choosing the single car accident will show a new window to choose one of the tools to start, see figure 4.22.

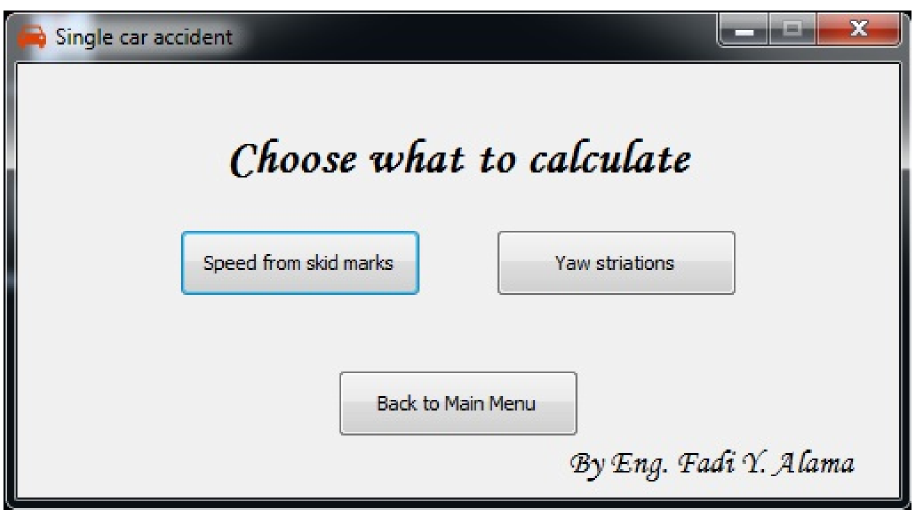

Figure 4.22: Single car accident window

Finally, many features were added to the program to prevent any bugs, such as prevent the user to move to the next window or to calculate with any empty box that he forgot to fill in, also preventing the user to write letters in a box that expected to receive numbers, etc. Also the user can clear the boxes by the clear button, and can move between the windows and methods quickly, and finally the user can go back to the home page window to insert a new accident data.

CHAPTER 5

CASE STUDY: HEAD-ON-COLLISION IN NEW JERSEY

Chapter 5

Case Study: Head-on-Collision in New Jersey

5.1 Introduction

In the previous chapters the methods of car accident reconstruction were discussed, and the program software was developed. In the present chapter a case study will be chosen and applied on the software that was developed as a verification example to discuss the results.

The police offices in Palestine were visited to find a case study, but unfortunately they don't have any technical report of any accident, because they don't have complete data and measurement from accident site. So the National Highway Traffic Safety Administration (NHTSA)[15] website were used to find a case study from the United States of America.

In the case study selection, some consideration were taken into account, the accident must be modern, the technical report must include enough data of the accident site and the vehicles and the results that they reached, so it could be reconstructed and discussed.

Consequently, the case study chosen has a Case No: 2004-04-069B, it was happened in July 2004, in New Jersey, between a Volkswagen-Passat-1999 and a Dodge-Ram-1999, and the accident type was head-on-collision[16]. The main needed technical data were extracted from the technical report and put in table 5.1 bellow, a copy of the NHTSA technical report is provided in Appendix A

Table 5.1: Technical report data for case study No: 2004-04-069B

Data	Vehicle 1	Vehicle 2
Vehicle maker	Volkswagen	Dodge
Vehicle model	Passat	Ram
Vehicle year	1999	1999
Vehicle weight (Kg)	1377	2053
Passengers total weight (Kg)	82	80
Cargo weight (Kg)	0	45
Total weight (Kg)	1459	2178
Collision Deformation Classification (CDC)	12-FDEW-3	12-FDEW-3
Length of deformation (m)	1.40	1.85
C1 (m)	0.68	0.53
C2 (m)	0.53	0.62
C3 (m)	0.41	0.65
C4 (m)	0.30	0.64
C5 (m)	0.23	0.49
C6 (m)	0.27	0.34
Pre-impact grade angle (λ_1 , λ_2)	+1.145	-1.145
Post-impact grade angle (λ_3 , λ_4)	-1.145	+1.145
Approach angle (α , β)	310	140
Departure angle (θ , γ)	100	350
ΔV (Km/hr)	66	44
Pre-impact speed (Km/hr)	43	59

Figure 5.1 shows the scene schematic for the accident site taken from the technical report.

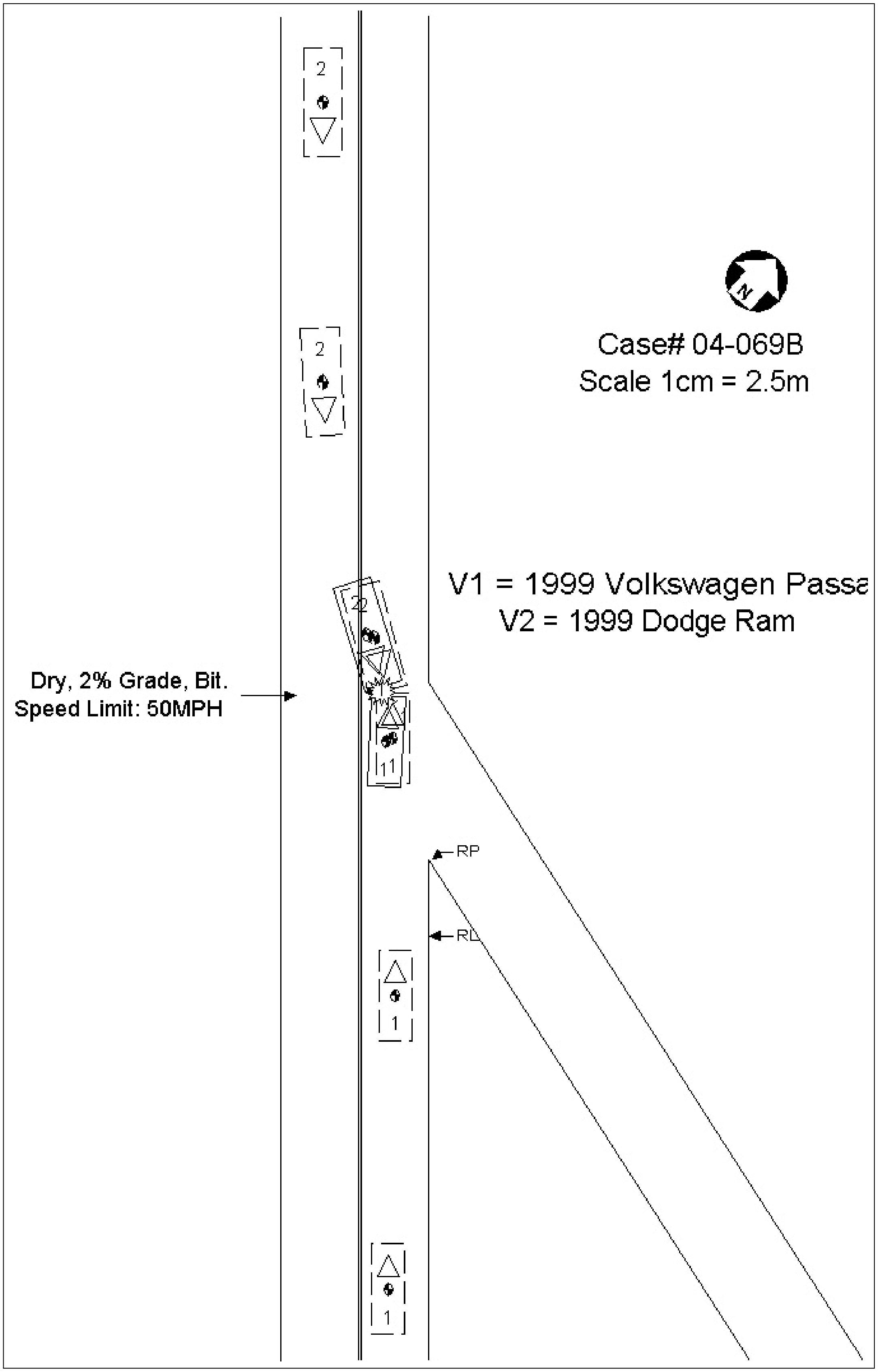

Figure 5.1: Scene schematic for the accident site[16]

5.2 Application of the developed methods on the case study

The combined method were used to reconstruct the case study. The extracted data from the technical report of the case study was enough, except the coefficient of stiffness A and B, and they were found in the ARAS company website[7], table 5.2 shows the coefficient of stiffness for the two vehicles.

Table 5.2: Coefficient of stiffness

Car	**Coefficient of stiffness**	
(maker-model-year)	**A** (N/m)	**B** (N/m^2)
Volkswagen - Passat - 1999 (Vehicle 1)	79497	602900
Dodge - Ram - 1999 (Vehicle 2)	68737	787811

In the next step the data of the case study were inserted in the program, the results obtained from the developed software are reported in table 5.3.

Table 5.3: Results of application the case study

Data	**Vehicle 1**	**Vehicle 2**
Vehicle maker	Volkswagen	Dodge
Vehicle model	Passat	Ram
Vehicle year	1999	1999
ΔV (Km/hr)	57	40
Pre-impact speed (Km/hr)	50	67
Post-impact speed (Km/hr)	19	28

5.3 Discussion

For discussing results the percentage of error (equation 5.1) will be calculated for the pre-impact speeds and the ΔV, between the NHTSA results in the technical report and the results obtained by the present study by the developed program. See figure 5.2.

$$error\% = \left(\frac{NHTSA_{value} - presentstudy_{value}}{NHTSA_{value}} \right) * 100\% \tag{5.1}$$

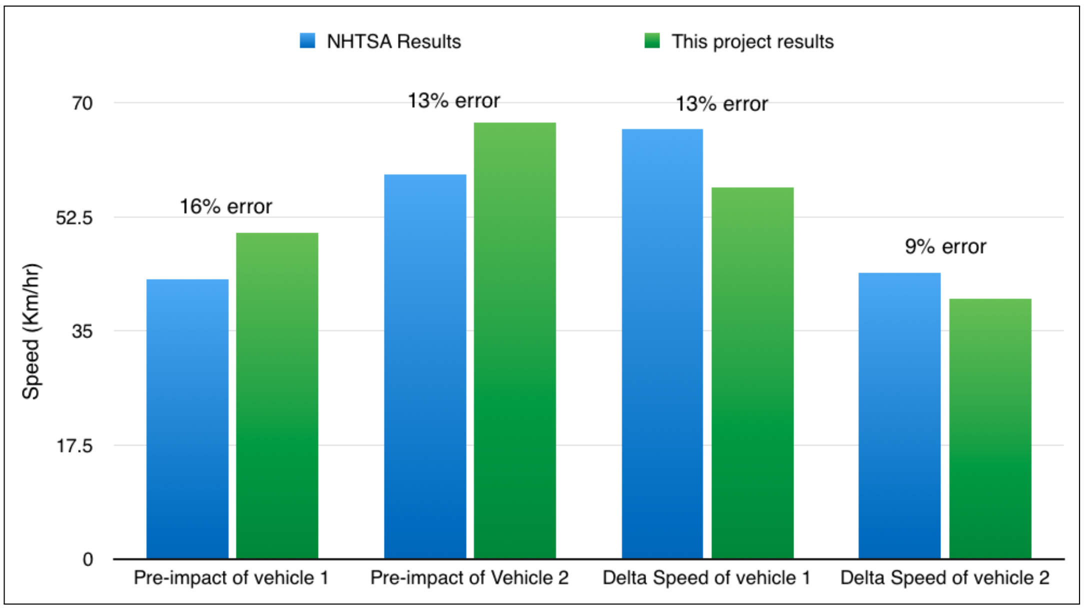

Figure 5.2: Results comparison

We found that the present study have a percent error in the range of $(9 - 16\%)$ compared with NHTSA results. The main reason for this error is the coefficient of stiffness of the vehicles, these coefficient calculation depends on the results of crash tests, and in the NHTSA report they were not mentioned, and they were collected from another reference, and this made this differences in the results. Also the vehicles selected for the crash test may have some differences compared to the real accident vehicles, even if they have the same model or year (for instance: long chassis and engine size). As a result we found that the combined method provided a good approximation of the results from NHTSA.

Moreover, we applied the other two methods (linear momentum and energy methods) on the selected case study to compare the results obtained by the three developed methods. The percent error was calculated by equation 5.2 and the results are reported in figure 5.3.

$$error\% = \left(\frac{V_{Combined\ method} - V_{Method}}{V_{Combined\ method}} \right) * 100\% \tag{5.2}$$

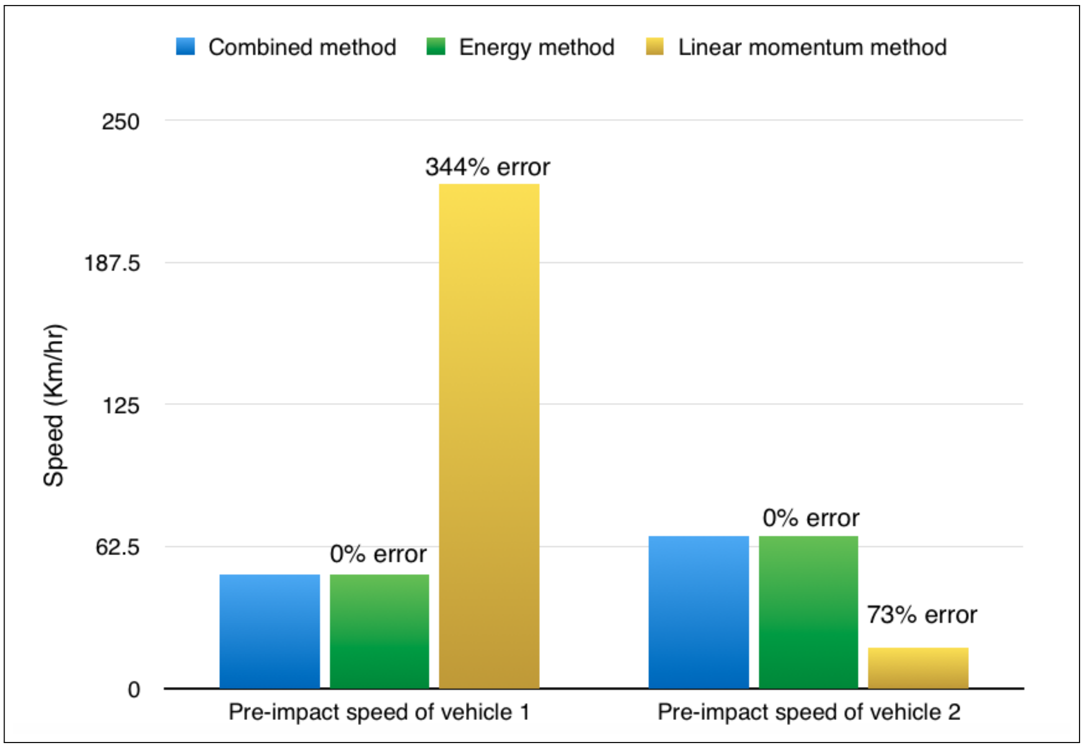

Figure 5.3: Methods comparison

The result of this comparison was that the energy method could work perfect, but the linear momentum could not. That because the linear momentum method does not include the energy losses in the deformation, and it consider that the car is an undeformable rigid body. Finally we concluded that the combined method is a good approach to analyze head-on-collision accident.

CHAPTER 6

CONCLUSION AND RECOMMENDATIONS

Chapter 6

Conclusion and Recommendations

6.1 Conclusion

Car accident site have many data that are valuable in car accident reconstruction to predict the speed of the vehicle before the accident. The purpose of this project was to review the available methods and develop methods and tools that can be used in the prediction of the vehicle speed before accident.

In this project the methods of conservation of linear momentum and energy were developed, and they were combined together to produce the combined method to reconstruct car to car accident. Also the road grade angle were added to the developed methods. And the tire marks tools were developed to reconstruct single car accident. Also a relation between car speed and risk of fatal was provided in this project.

Moreover, we developed two versions for the car accident reconstruction software using Matlab and C-sharp programs, a developer interface version for researchers and developers, and a user interface version for direct use by users to analyze real accident data.

The developer interface version include all methods and tools that can help the developer to modify and develop the methods and the software, and the user interface version include the methods that have been used in the case study which is the combined method for a direct use.

The police offices in Palestine were visited to find a case study, but unfortunately they don't have any technical report of any accident, because they don't have complete data and measurement from accident site. So the National Highway Traffic Safety Administration (NHTSA)[15] website were used to find a case study from the United States of America, and this case study was added in this project as a verification example for the developed methods.

The case study was selected is a head-on-collision accident between two cars in New Jersey. And it was inserted in the developed software. Then the results were compared with the NHTSA real results and we reached to a percent error in the range of $(13-16\%)$ for the pre-impact vehicle speed, and a percent error in the range of $(9-13\%)$ for the change of speed (ΔV) for each vehicle.

Then the three developed methods were compared together to found that the combined method is the most powerful method to reconstruct head-on-collision accident, as well the energy method if the vehicle have the EDR device. But the linear momentum method produce wrong reconstruction if it used alone, because it does not include the energy losses in deformation and it consider that the vehicle is an undeformable rigid body.

Finally the output of this project is a user interface software that can reconstruct a single car accident, and a head-on-collision accident. And the main software which is the developer interface version that can be used in the future to develop the methods and tools to handle different accident types (for example: rear-end-collision, side-impact-collision and multi-car-collision).

6.2 Recommendation

At the end of this project some recommendations will be mentioned.

- Our recommendation for the university is to register in car accident reconstruction developer organizations such as ARAS company and Crash3 program to help the students to find the data they need for the reconstructed vehicles such as the coefficient of stiffness. Also we recommend to organize specialize training workshops in car accident reconstruction for the police officers to discuss all needed data they have to collect from the accident site, and how to use it in the developed software to have a good prediction for the pre-impact vehicle speed, and how to make a technical report for each accident. Moreover, to make a Joint cooperation between the Mechanical, Computer and Graphics Departments in Palestine Polytechnic University to develop our software to include video simulation.
- For student in the future work, we recommend to collect new case studies for different accident types (for example: rear-end-collision and side-impact-collision) to ensure that the combined method can handle these types. Also to develop the combined method to reconstruct multi-car-collision. For reducing the percent error we have reached, we recommend to develop the car model from a moving particle to the quarter car model. Finally, to study the methods of calculating the coefficient of stiffness to choose the most accurate method, so that will reduce the percent of error.

REFERENCES

[1] Nosmut. List of road accidents on nosmut(dot)com, the siev, 2014. http://nosmut.com/List_of_road_accidents.html.

[2] Association for safety international Road travel. Road crash statistics, 2015. http://asirt.org/Initiatives/Informing-Road-Users/Road-Safety-Facts/Road-Crash-Statistics.

[3] International Trnsport Forum. Passenger transport, 2014. http://stats.oecd.org/Index.aspx?DataSetCode=ITF_PASSENGER_TRANSPORT#.

[4] PE Wade Bartlett. Conservation of linear momentum (COLM). *Pennsylvania State Police Annual Reconstruction Conference*, 2005.

[5] R.A. Serway and J.W. Jewett. *Physics for scientists and engineers: Raymond A. Serway, John W. Jewett, Jr.* Number v. 2 in Physics for Scientists and Engineers: Raymond A. Serway, John W. Jewett, Jr. Thomson-Brooks/Cole, 2004.

[6] Nicholas S Tumbas and Russell A Smith. Measuring protocol for quantifying vehicle damage from an energy basis point of view. Technical report, SAE Technical Paper, 1988.

[7] ARAS360HD. Vehicle stiffness - database, 2015. `http://www.aras360.com/resources/vehicle-stiffness-database.html`.

[8] Transport Research Laboratory of the Department for Transport in London. Relationship between speed and risk of fatal injury: Pedestriansand car occupants. *Road Safety Web Publication No.16*, 2010.

[9] James O. Harris. Determining vehicle speed from skid marks. *Internal Report*.

[10] *Maths delivers Braking distance*. The University of Melbourne on behalf of the Australian Mathematical Sciences Institute (AMSI), 2011.

[11] Technology Associates Engineering Experts. Reaction time in accident reconstruction, 2015. `http://www.technology-assoc.com/articles/reaction-time.html`.

[12] Queensland Government Department of Transport and Main Roads. Stopping distances (department of transport and main roads), 2015. `http://www.tmr.qld.gov.au/Safety/Driver-guide/Speeding/Stopping-distances.aspx`.

[13] Gray Beauchamp, David Hessel, Nathan A Rose, Stephen J Fenton, and Tilo Voitel. Determining vehicle steering and braking from yaw mark striations. Technical report, SAE Technical Paper, 2009.

[14] T.D. Gillespie. *Fundamentals of Vehicle Dynamics*. Society of Automotive Engineers, 1992.

[15] National Highway Traffic Safety Administration (NHTSA). Special crash investigations, 28-July-2015. `http://www-nass.nhtsa.dot.gov/nass/sci/SearchForm.aspx?ClearSearch`.

[16] National Highway Traffic Safety Administration (NHTSA). Sci case viewer (case number: 2004-04-069b), 2004. http://www-nass.nhtsa.dot.gov/nass/sci/CaseForm.aspx?xsl=main.xsl&CaseID=817662808.

Appendices

APPENDIX A

NHTSA TECHNICAL REPORT

CASE NO: 2004-04-069B

TRANSPORTATION SCIENCES
CRASH DATA RESEARCH CENTER

Advanced Information Engineering Services
A General Dynamics Company
Buffalo, NY 14225

GENERAL DYNAMICS REMOTE CHILD SAFETY SEAT INVESTIGATION

NASS/SCI COMBO CASE NO: 04-04-069B

VEHICLE: 1999 VOLKSWAGEN PASSAT

LOCATION: NEW JERSEY

CRASH DATE: JULY 2004

Contract No. DTNH22-01-C-17002

Prepared for:

U.S. Department of Transportation
National Highway Traffic Safety Administration
Washington, D.C. 20590

DISCLAIMER

This document is disseminated under the sponsorship of the Department of Transportation in the interest of information exchange. The United States Government assumes no responsibility for the contents or use thereof.

The opinions, findings, and conclusions expressed in this publication are those of the authors and not necessarily those of the National Highway Traffic Safety Administration.

The crash investigation process is an inexact science which requires that physical evidence such as skid marks, vehicular damage measurements, and occupant contact points are coupled with the investigator's expert knowledge and experience of vehicle dynamics and occupant kinematics in order to determine the pre-crash, crash, and post-crash movements of involved vehicles and occupants.

Because each crash is a unique sequence of events, generalized conclusions cannot be made concerning the crashworthiness performance of the involved vehicle(s) or their safety systems.

TECHNICAL REPORT STANDARD TITLE PAGE

1. Report No. 04-04-069B	*2. Government Accession No.*	*3. Recipient's Catalog No.*
4. Title and Subtitle General Dynamics Remote Child Safety Seat Investigation Vehicle: 1999 Volkswagen Passat Location: State of New Jersey		*5. Report Date*: December 2004 *6. Performing Organization Code*
7. Author(s) Crash Data Research Center		*8. Performing Organization Report No.*
9. Performing Organization Name and Address Transportation Sciences Crash Data Research Center Advanced Information Engineering Services A General Dynamics Company P.O. Box 400 Buffalo, New York 14225		*10. Work Unit No.* C00410.0000.0222 *11. Contract or Grant No.* DTNH22-01-C-17002
12. Sponsoring Agency Name and Address U.S. Department of Transportation National Highway Traffic Safety Administration Washington, D.C. 20590		*13. Type of Report and Period Covered* Technical Report Crash Date: July 2004 *14. Sponsoring Agency Code*

15. Supplementary Note

On-site investigation focused on the performance of a child safety seat and the fatal injuries sustained by the child occupant.

16. Abstract

This remote investigative effort focused on the performance of the Belt Positioning Booster (BPB) seat and the resulting injury mechanisms of the child occupant of a 1999 Volkswagen Passat. The Volkswagen was involved in a head-on collision with a 1999 Dodge Ram pickup truck. The Volkswagen was occupied by a restrained 25-year-old female driver and a 3-year-old female positioned in a BPB and restrained by the vehicle's lap and shoulder safety belt in the rear left. The Dodge was occupied by a 39-year-old male driver. The driver of the Dodge initiated a left turn at a Y-intersection which resulted in the head-on collision with the Volkswagen. The impact resulted the frontal air bag deployment in the Passat and the firing of the safety belt pretensioners in the four outboard positions. The 25-year-old female driver of the Volkswagen sustained police reported internal abdominal bleeding and was transported to a trauma center. The medical records for the driver were not obtained due to lack of a medical release and cooperation by the driver. Therefore, the specific injuries and treatment were unknown. The 3-year-old female passenger of the Volkswagen sustained serious level injures and was transported to a local hospital where she was airlifted to a trauma center. The 3-year-old female expired prior to arrival at the trauma center. The driver of the Dodge sustained minor injuries and was transported to a hospital where he was treated and released.

17. Key Words Belt Positioning Booster Seat Frontal Air Bag Deployment		*18. Distribution Statement* General Public	
19. Security Classif. (of this report) Unclassified	*20. Security Classif. (of this page)* Unclassified	*21. No. of Pages* 15	*22. Price*

TABLE OF CONTENTS

GENERAL DYNAMICS REMOTE CHILD SAFETY SEAT INVESTIGATION
NASS/SCI COMBO CASE NO.: 04-04-69B
LOCATION: STATE OF NEW JERSEY
VEHICLE: 1999 VOLKSWAGEN PASSAT
CRASH DATE: JULY 2004

BACKGROUND

Figure 1. Subject vehicle 1999 Volkswagen Passat.

This remote investigative effort focused on the performance of the Belt Positioning Booster (BPB) seat and the resulting injury mechanisms of the child occupant of a 1999 Volkswagen Passat **(Figure 1)**. The Volkswagen was involved in a head-on collision with a 1999 Dodge Ram pickup truck. The Volkswagen was occupied by a restrained 25-year-old female driver and a 3-year-old female positioned in a BPB and restrained by the vehicle's lap and shoulder safety belt in the rear left. The Dodge was occupied by a 39-year-old male driver. The driver of the Dodge initiated a left turn at a Y-intersection which resulted in the head-on collision with the Volkswagen. The impact resulted the frontal air bag deployment in the Passat and the firing of the safety belt pretensioners in the four outboard positions. The 25-year-old female driver of the Volkswagen sustained police reported internal abdominal bleeding and was transported to a trauma center. The medical records for the driver were not obtained due to lack of a medical release and cooperation by the driver. Therefore, the specific injuries and treatment were unknown. The 3-year-old female passenger of the Volkswagen sustained serious level injures and was transported to a local hospital where she was airlifted to a trauma center. The 3-year-old female expired prior to arrival at the trauma center. The driver of the Dodge sustained minor injuries and was transported to a hospital where he was treated and released.

This crash was identified by the National Automotive Sampling System (NASS) PSU 04 during the weekly sampling of Police Accident Reports (PARs). This crash was selected and researched as CDS Case No. 04-04-069B. The NASS PSU performed the vehicle, scene and child safety seat inspections. Due to the presence of the child safety seat and the fatal injuries sustained by the child occupant in the 1999 Volkswagen Passat, NHTSA assigned the tasks of case review and report preparation to the General Dynamics SCI team.

SUMMARY

Crash Site

This intersection crash occurred during the evening hours of July 2004. At the time of the crash, it was daylight and the asphalt road surface was dry. The crash occurred at an angled three-leg intersection. The east/westbound roadway was configured with one travel lane in each direction and was delineated by a double yellow centerline. A concrete barrier curb bordered the south road edge. The intersecting roadway was configured with two travel lanes that were not delineated. Traffic flow through the intersection was not controlled. The posted speed limit for the east/westbound roadway was 80 km/h (50 mph). The NASS scene schematic is included as **(Figure 15)** of this report.

Vehicle Data – 1999 Volkswagen Passat

The 1999 Volkswagen Passat was identified by the Vehicle Identification Number (VIN): 3B7HC12YXX (production sequence omitted). The vehicle was a four-door sedan that was equipped with a 1.8-liter turbo, I4 engine linked to a four-speed automatic transmission, 4-wheel power disc brakes with antilock, power steering, and a tilt/telescoping steering wheel. At the time of the vehicle inspection, the odometer could not be read due to the lack of power to the vehicle. The manufacturers recommended tire pressure was unknown, the NASS researcher could not locate the vehicle placard. The Volkswagen was configured with Hercules tires size P195/65R15. The specific tire data was as follows:

Position	Measured Pressure	Tread Depth	Restricted	Damage
LF	0 kpa	6 mm (8/32)	Yes	Unknown
LR	200 kpa (29 psi)	7 mm (9/32)	No	None
RF	234 kpa (34 psi)	6 mm (8/32)	No	None
RR	200 kpa (29 psi)	7 mm (9/32)	No	None

The Volkswagen was configured with front bucket seats with height adjustable head restraints. The driver's head restraint was adjusted between the mid to full-down position. The front right head restraint was adjusted to the full-down position. The second row was configured with a three-passenger bench seat with a split, forward folding seatback (60/40). The outboard seats were equipped with height adjustable head restraints that were adjusted to the full-down position.

1999 Dodge Ram

The 1999 Dodge Ram was identified by the Vehicle Identification Number (VIN): 3B7HC12YXX (production sequence omitted). The vehicle was a two-door pickup truck that was equipped with a 5.2 liter, V8 engine linked to a four-speed automatic transmission, power brakes, power steering, and a tilt steering wheel. At the time of the vehicle inspection the odometer could not be read due to the lack of power to the vehicle. The Dodge was equipped with Goodyear tires in the front and General tires on the rear size P245/75R16. The vehicle manufacturers recommended tire size was P225/75R16 with a recommended tire pressure of 283.0 kPa (41.0 PSI) for the front and rear tires. The specific tire data was as follows:

Position	Measured Pressure	Tread Depth	Restricted	Damage
LF	296 kpa (43 psi)	7 mm (9/32)	Yes	None
LR	179 kpa (26 psi)	3 mm (4/32)	No	None
RF	324 kpa (47 psi)	5 mm (6/32)	No	None
RR	324kpa (47 psi)	3 mm (4/32)	No	None

Crash Sequence

Pre-Crash

The 25-year-old female driver of the Volkswagen was operating the vehicle in a westbound **(Figure 2)** direction on the two-lane roadway approaching a three-leg Y-intersection. The 39-year-old male driver of the Dodge was operating the vehicle eastbound **(Figure 3)** on the same roadway approaching the same intersection. As the driver of the Dodge continued his eastbound travel, he initiated a left turn prior to the intersection and entered the westbound travel lane.

Figure 2. Volkswagen's westbound approach.

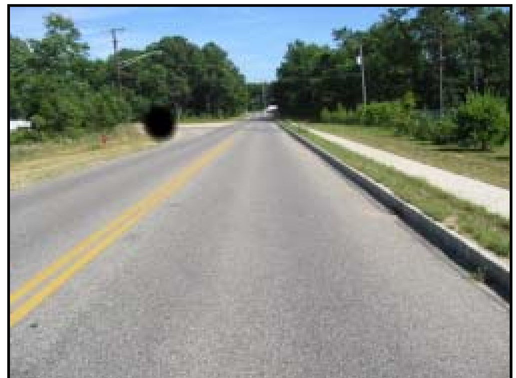

Figure 3. Dodge's eastbound approach.

Crash

The full frontal aspect of the Dodge impacted the full frontal aspect of the Volkswagen in the intersection. The impact resulted in severe frontal damage to the Volkswagen and the Dodge. The resultant directions of force were within 12 o'clock for both vehicles. The WINSMASH damage algorithm was used to calculate a delta for this impact. The total calculated delta V for the Volkswagen was 66.0 km/h (41.0 mph). The longitudinal and lateral components were -65.0 km/h (40.4 mph) and 11.5 km/h (7.1 mph), respectively. The total calculated delta V for the Dodge was 44.0 km/h (27.3 mph). The longitudinal and lateral components were -43.3 km/h (-26.9 mph) and -7.6 km/h (-4.7 mph), respectively. The impact resulted in the frontal air bag deployment and pretensioner firing in the Passat. The vehicles came to rest with the intersection.

Post-Crash

Police and EMS personnel responded to the crash site. The 25-year-old female driver of the Volkswagen sustained police reported internal abdominal bleeding and was transported by ambulance to a regional trauma center. The 3-year-old female passenger of the Volkswagen sustained serious level injures and was transported to a local hospital where she was airlifted to a trauma center. The 3-year-old female expired prior to arrival at the trauma center. The driver of the Dodge sustained minor injuries and was transported to a hospital where he was treated and released. Both vehicles sustained severe damage and were towed from the crash site.

Vehicle Damage

Exterior Damage – 1999 Volkswagen Passat

The 1999 Volkswagen Passat sustained severe severity frontal damage as a result of the impact with the Dodge **(Figure 4)**. The direct contact damage began at the front left bumper corner and extended 140.0 cm (55.1") to the front right bumper corner. The maximum crush was located at the front left bumper corner and measured 68.0 cm (26.8"). The damage resulted in the longitudinal displacement of the frontal components. The NASS researcher used six equidistant measurements to document the crush at the bumper level using a combined direct and induced damage width of 140.0 cm (55.5") and were as follows: C1 = 68.0 cm (26.8"), C2 = 53.0 cm (20.9"), C3 = 41.0 cm (16.1"), C4 = 30.0 cm (11.8"), C5 = 23.0 cm (9.1"), C6 = 27.0 cm (10.6"). The Collision Deformation Classification (CDC) for this impact was 12-FDEW-3.

Figure 4. Resultant frontal damage to the Volkswagen.

Interior Damage – 1999 Volkswagen Passat

The 1999 Volkswagen Passat sustained moderate damage as a result of occupant contacts. At impact with the Dodge, the frontal air bags deployed. The air bag deployment resulted in the displacement of the driver's left arm. As a result of this displacement, the driver's upper left arm contacted the front left window frame which was evidenced by hair. The driver's lower left arm contacted the door panel mounted power mirror control that was fractured. The NASS researcher noted a scuffmark to the knee bolster from contact with the driver's left knee. Also noted was stretching to the lap belt portion of the safety belt from the driver's abdomen loading the safety belt.

Figure 5. Overall view of the driver's area.

The 3-year-old female rear left passenger was seated in a belt-positioning booster at the time of the crash. At impact with the Dodge, she initiated a forward trajectory and loaded the shoulder portion of the manual 3-point lap and shoulder belt. The NASS researcher noted stretching and scratching to the safety belt webbing from the occupant contact/loading. **Figures 5 and 6** are overall views of the left side first and second rows.

Figure 6. Overall view of the second row left side.

The Volkswagen sustained moderate damage as a result of passenger compartment intrusion. The intrusions are listed in the following table:

Seat Position	Intruded Component	Magnitude	Direction
Front left	Windshield	9.0 cm (3.5”)	Longitudinal
Front left	Roof side rail	6.0 cm (2.4”)	Vertical
Front left	Roof	5.0 cm (1.9”)	Vertical
Front left	Toe pan	14.0 cm (5.5”)	Longitudinal
Front left	Left instrument panel	10.0 cm (3.9”)	Longitudinal
Front center	Windshield	17.0 cm (6.7”)	Longitudinal
Front center	Center instrument panel	6.0 cm (2.4”)	Lateral
Front right	Windshield	14.0 cm (5.5”)	Longitudinal
Front right	Toe pan	9.0 cm (3.5”)	Longitudinal
Rear left	B-pillar	3.0 cm (1.2”)	Lateral
Rear left	Floor	10.0 cm (3.9”)	Vertical
Rear right	Floor	10.0 cm (3.9”)	Vertical

Exterior – 1999 Dodge Ram

The 1999 Dodge Ram pickup truck sustained severe frontal damage as a result of the impact with the Volkswagen **(Figures 7)**. The direct damage began at the front left bumper corner and extended 185.0 cm (72.8”) to the right bumper corner. The maximum crush was located at the center of the frontal bumper and measured 65.0 cm (25.6”). Six crush measurements were used to document the crush along the frontal plane at the bumper level using a combined direct and induced damage width of 185.0 cm (72.8”) and were as follows: C1 = 53.0 cm (20.8”), C2 = 62.0 cm (24.4”), C3 = 65.0 cm (25.6”), C4 = 64.0 cm (25.2”), C5 = 49.0 cm (19.3”), C6 = 34.0 cm (13.4”). The CDC for this impact was 12-FDEW-3.

Figure 7. Crush profile for the 1999 Dodge Ram.

Manual Restraints Systems – 1999 Volkswagen Passat

The 1999 Volkswagen Passat was configured with manual 3-point lap and shoulder belts for the four outboard seating positions. The driver's safety belt **(Figure 8)** was configured with continuous loop webbing, sliding latch plate, height adjustable D-ring that was in the lower position at the time of the NASS inspection, Emergency Locking Retractor (ELR), and a retractor pretensioner that fired as a result of the crash. The stretching to the lap belt portion of the safety belt resulted from the driver's pelvic region loading the safety belt. Minimal occupant contacts and the fired status of the pretensioner supported the safety belt usage for the driver. The front right safety belt was configured with a sliding latch plate, height adjustable D-ring that was in the lower position at the time of the NASS inspection, switchable ELR/Automatic Locking Retractor (ALR), and a retractor pretensioner that did not fire.

Figure 8. Driver's safety belt.

The second row outboard safety belts were configured with sliding latch plates, switchable ELR/Automatic Locking Retractor (ALR), and retractor pretensioners that fired as a result of the crash. The rear left safety belt **(Figure 9)** was used with a high back belt-positioning booster seat which was supported by the stretching and scratching to the safety belt from the occupant contact/loading and fired retractor pretensioner. The rear right safety belt was used to restrain an unoccupied belt positioning booster seat at the time of the crash, which was evidenced by the fired retractor pretensioner. The rear center safety belt was a 2-point manual lap belt that was configured with a sliding latch plate and an ALR.

Figure 9. Rear left safety belt with fired pretensioner.

High-Back Belt Positioning Booster Child Safety Seat– Cosco Complete Voyager

The Cosco Complete Voyager high-back Belt-Positioning Booster (BPB) seat **(Figures 10 and 11)** was identified by the Model Number: 22-210-TIM. The date of manufacture was March 5, 2004. The BPB was configured with three shoulder belt positioning slots on the upper outboard aspects. It was not known what position the shoulder belt was placed. It should be noted that use of the shoulder belt positioners could not be confirmed. The NASS researcher noted a stress crease on the rear aspect of the right side panel of the of BPB. Also noted was a spot of body fluid on the upper right side of the seatback and a scuff to the lower right side of the cushion. The manual 3-point lap and shoulder belt was used to restrain the child in the rear left seat of the vehicle. The vehicle's safety belt system was equipped with a retractor pretensioner that fired as a result of the crash. The safety belt was found restricted in the used position which was as result of the fired pretensioner. The BPB was used to position the 3-year-old child to ensure a proper fit with the vehicle's safety belt. A label on the BPB outlined the recommended use of the BPB as follows:

Belt-Positioning Booster

- Use only with children who weigh between 14-36 kg (30-80 lb) and height is between 73-132 cm (29-52") and over 1 year in age.

Do not use this child restraint if the midpoint of your child's head is above the top of the child restraints seatback.

- Use only the vehicle's lap and shoulder belt system when restraining the child in this booster seat.
- Do not use with lap belt only

Figure 10. BPB in the vehicle's rear left position.

Figure 11. Overall view of BPB.

Unoccupied High-Back Belt Positioning Booster Child Safety Seat – Cosco Complete Voyager

The NASS researcher noted a second BPB **(Figure 12)** in the rear right position of the Volkswagen. This BPB was not occupied at the time of the crash. The BPB was a Cosco Complete Voyager with a model number of 22-210-TM. The date of manufacture for this BPB was November 13, 2003. The BPB was found with the manual 3-point lap and shoulder belt in the used position. This was supported by the fired retractor pretensioner.

Figure 12. Unoccupied BPB.

Redesigned Frontal Air Bag System – 1999 Volkswagen Passat

The 1999 Volkswagen Passat was equipped with redesigned frontal air bags for the driver and front right passenger positions. The driver's air bag was conventionally located in the center of the steering wheel and the front right passenger's air bag was a top-mount module located on the right instrument panel. The redesigned frontal air bag system deployed as result of the subject crash.

Figure 13. Deployed driver's frontal air bag.

The driver's air bag module consisted of two H-configuration cover flaps. The top cover flap measured 17.0 cm (6.7") in width and 9.0 cm (3.5") in height. The lower cover flap measured 17.0 cm (6.7") in width and 7.0 cm (2.8") in height. The driver's air bag measured 72.0 cm (28.3") in diameter in its deflated state and contained two tethers. A single vent port that was located at the 12 o'clock position on the rear aspect vented the air bag. The NASS researcher noted no occupant contacts or failures to the driver's air bag. **Figure 13** is an overall view of the deployed driver's frontal air bag.

Figure 14. Deployed front right air bag.

The front right air bag **(Figure 14)** module consisted of a single cover flap configuration that measured 34.0 cm (13.4") in width and 20.0 cm (7.9") in height. The air bag membrane measured 70.0 cm (27.8") in width and 85.0 cm (33.5") in height and was not tethered. A single vent port that was located at the 11 o'clock position on the rear aspect of the top panel vented the air bag. No occupant contacts or failures were noted to the front right air bag.

Side impact Air Bags – 1999 Volkswagen Passat

The 1999 Volkswagen Passat was equipped with seatback mounted side impact air bags for the front seating positions. The side impact air bags did not deploy in the subject crash.

Occupant Demographics – 1999 Volkswagen Passat

Driver

Age/Sex:	25-year-old female
Height:	Unknown
Weight:	Unknown
Seat Track Position:	Forward track
Manual Restraint Use:	Manual 3-point lap and shoulder belt
Usage Source:	Vehicle inspection
Eyewear:	Unknown
Type of Medical Treatment:	Transported to a regional trauma center, unknown type of treatment.

Driver Kinematics

The 25-year-old female driver of the Volkswagen was seated in a presumed upright posture with the seat track adjusted to a forward track position. At impact with the Dodge, the driver's frontal air bag deployed. The air bag expanded against her left anterior forearm which displaced driver's left arm from the steering wheel rim. As a result of this displacement, the driver's left forearm contacted the front left window frame which was evidenced by hair. The driver's left elbow contacted and fractured the door panel mounted power mirror control. The driver was displaced forward as result of the 12 o'clock impact force. The forward movement resulted in stretching to the lap belt portion of the safety belt from the driver's pelvic region loading the safety belt. Also noted was a scuff to the knee bolster from contact with the driver's left knee.

As a result of the crash, the driver sustained police reported internal abdominal bleeding and was transported by ambulance to a regional trauma center. The medical records for the driver were not obtained due to lack of a medical release and cooperation by the driver. Therefore, the specific injuries and treatment were unknown.

Rear Left Passenger

Age/Sex:	3-year-old female
Height:	99.0 cm (40.0”)
Weight:	17 kg (37 lb)
Seat Track Position:	Not adjustable
Manual Restraint Use:	Belt positioning booster seat Cosco Complete Voyager with vehicle’s lap and shoulder belt
Usage Source:	Vehicle inspection, CSS inspection
Eyewear:	Unknown
Type of Medical Treatment:	Transported to a hospital by ambulance and then was airlifted to a trauma center where she expired on route.

Rear Left Passenger Injuries

Injury	Injury Severity (AIS 90/Update 98)	Injury Source
Small cerebrum subarachnoid hemorrhage (posterior surfaces)	Serious (140684.3,9)	BPB seatback
Small cerebellum subarachnoid hemorrhage	Serious (140466.3,6)	BPB seatback
Mild cerebrum swelling	Serious (140662.3, 3)	Hyperflexion
Thoracic cavity injury with hemo-/pneumothorax	Serious (442202.3,2)	Shoulder belt
Upper cervical spine fracture with atlanto-occipital subluxation (dislocation)	Moderate (650216.2,6)	Hyperflexion
Jenjunum-ileum contusion (upper small intestines)	Moderate (541410.2,8)	Lap belt
Mesentery contusion	Moderate (542010.2,8)	Lap belt
Inferior abdomen contusion	Minor (590402.1,8)	Lap belt
12.7 x 3.8 cm (5.0 x 1.5”) contusion of the upper left chest and left anterior shoulder	Minor (490402.1,2), (790402.1,2)	Shoulder belt

Injury source: Autopsy

Rear Left Passenger Kinematics

The 3-year-old female passenger was restrained in a Cosco Complete Voyager high-back BPB on the left aspect of the second row bench seat. At impact with the Dodge, she initiated a forward trajectory and her upper body loaded the manual 3-point lap and shoulder belt. This loading resulted in the thoracic cavity injury with hemo-/pneumothorax, jenjunum-ileum contusion, mesentery contusion, inferior abdomen contusion, and a 12.7x3.8 cm (5.0x1.5”) contusion of the upper left chest and left anterior shoulder.

The loading of the safety belt restricted the movement of the passenger's torso which allowed her head to hyperflex over the shoulder belt portion of the safety belt. This hyperflexion resulted in the mild cerebrum swelling, upper cervical spine fracture with atlanto-occipital subluxation. The 3-year-old passenger rebounded into the BPB and her head contacted the upper aspect of the BPB seatback, which resulted in the small cerebrum subarachnoid hemorrhage and small cerebellum subarachnoid hemorrhage.

Medical Treatment

The 3-year-old passenger was transported by ambulance to a local hospital where she was airlifted to a trauma center. The 3-year-old female expired prior to the arrival at the trauma center. The medical records for the initial hospital were not obtained due to lack of a medical release and cooperation by the driver.

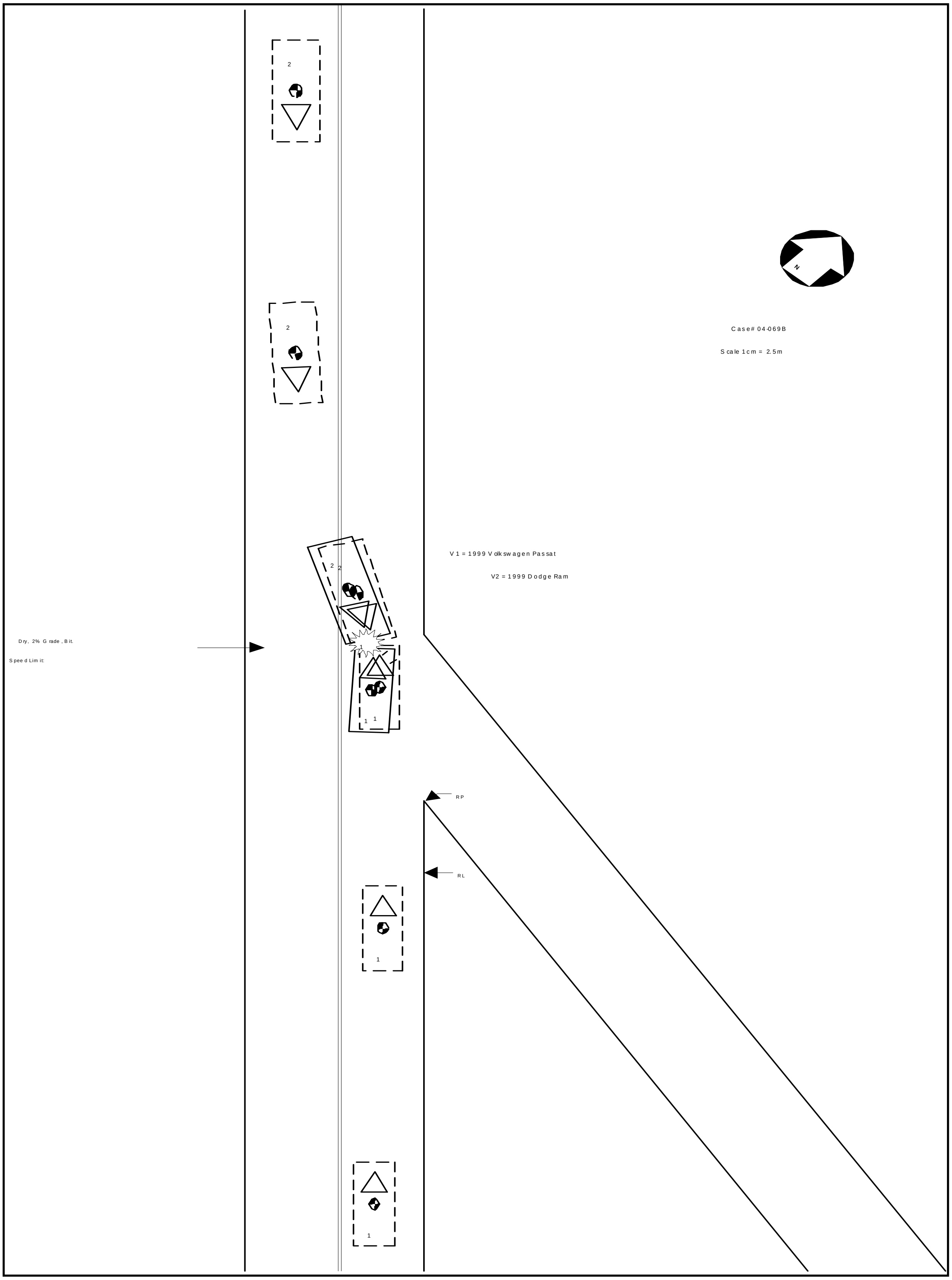

Figure 15. Scene Schematic